BACTERIALLY-INDUCED DISSOLUTION OF CALCITE: THE ROLE OF BACTERIA IN LIMESTONE WEATHERING

Fatimah SULU-GAMBARI
Department of Earth & Planetary Science, McGill

May 2011

A Thesis Submitted to McGill University in Partial Fulfillment of the Degree of Master of Science

Abstract

The interaction between microorganisms and the calcite mineral surface in aqueous solutions, under earth surface conditions, was the focus of this study. More specifically, we investigated if bacterial attachment and metabolism increase the dissolution rates of calcite crystals and alter their surfaces in solution. A natural microbial consortium, rather than model organisms, was used in the experiments. Weathered samples from the Trenton carbonates were collected on the flanks of Mount Royal in Montréal (Québec, Canada). The associated bacteria were identified using molecular biology DNA fingerprinting techniques. This information was used to determine the nutrient requirements of suitable growth media. Samples contained typical soil dwelling organisms from the phylum *Actinobacteria*, gram-positive heterotrophs. Bacteria were combined with cleaved Iceland Spar calcite rhombohedra in a low-ionic strength (10^{-2} M) NaCl solution at ambient pCO_2, 25 °C and 1 atm pressure. The effect of solution chemistry (e.g. the presence of phosphate) on the calcite dissolution kinetics was also investigated. The dissolution rates in the presence of bacteria did not vary significantly from abiotic conditions, but decreased notably in the presence of phosphate.

keywords calcite, bacteria, dissolution kinetics, saturation state, phosphate

Résumé

Cette étude porte sur les interactions entre des micro-organismes et la surface de la calcite en solution aqueuse sous des conditions équivalentes à celles de la surface de la terre. Plus précisément, nous avons étudié si l'attachement des bactéries et leur métabolisme augmentent la vitesse de dissolution des cristaux de calcite et altérent leur surface en solution. Des communautés microbiennes naturelles ont été privilégiées à des organismes types pour les expériences. Des échantillons altérés provenant de carbonates de Trenton ont été récoltés sur les flancs du Mont Royal à Montréal (Québec, Canada). Les bactéries associées ont été identifiées par des techniques de biologie moléculaire utilisant leurs empreintes génétiques d'ADN. Ces informations ont servi à déterminer les besoins en nutriments des milieux de croissance. Les échantillons contenaient des organismes typiques de sols, hétérotrophes, à gram positif, du phylum *Actinobacteria*. Les bactéries ont été combinées avec des rhombohèdres clivés de calcite provenant de spaths d'Islande dans une solution de NaCl de faible force ionique (10^{-2} M) à pCO_2 ambiante, 25 °C et 1 atm de pression. L'effet de la composition chimique de la solution sur la cinétique de dissolution des calcites (en particulier, la présence de phosphate) a également été étudié. Les vitesses de dissolution en présence de bactéries ne varient pas de façon significative comparativement aux échantillons exposés aux conditions abiotiques. En revanche, la présence de phosphate dans le milieu de culture masque l'effet des bactéries sur la vitesse de dissolution.

mots-clés calcite, bactéries, cinétique de dissolution, état de saturation, phosphate

Contents

Dedication

What is of all things most yielding,
Can overcome that which is most hard (Lao Tzu)

To my families, to my loved-ones, to my friends; in no particular order of importance.

Preface and Contribution of Authors

The experimental design was guided by Alfonso Mucci and Dominic Frigon and implemented by the main author. Microbe characterisation analyses were conducted by the main author, under the supervision of Dominic Frigon. Dissolution experiments were completed by the main author. Microscopy to observe bacterial attachment was conducted by the main author with the assistance of Dominic Frigon.

This thesis consists of 4 chapters. Chapter 1 presents a general introduction to the study and objectives, supplemented by a review of mechanisms of mineral dissolution. Chapter 2 is a literature review on bacteria-mediated mineral dissolution, including a selection of reports on similar laboratory research. Chapter 3 is a manuscript on the empirical study of bacterial dissolution of calcite. It includes a description of the methods and experimental design employed in, as well as the results acquired from the study. Modelling using hydrogeochemical and chemical speciation programmes like PHREEQC, is also described as a theoretical reference point and/or comparison for the methods used and the results obtained. Chapter 4 presents a summary of the findings and implications of the study.

Acknowledgements

Gratitude is extended to the following people for their assistance, advice, editing and contributions to this study and to the compilation of my thesis.

Supervisors Alfonso Mucci and Dominic Frigon for their corrections and recommendations.

Faculty Bjorn Sundby (McGill) and Boswell Wing (McGill) for the use of their laboratory facilities.

Lab technicians Constance Guignard (McGill) for assistance with the coulometer, spectrophotometer, titrators and for her general guidance and knowledge about analytical techniques. Glenna Keating (McGill) and Isabelle Richer (McGill) for assistance with AAS and XRF. Jean-François Hélie (UQAM) and Agnieszka Adamowicz (UQAM) for their assistance with the total Carbon and Nitrogen analyses. Michel Préda (UQAM) for assistance with XRD analysis. Line Mongeon (McGill) for assistance with FEG-SEM.

Colleagues Dirk Schumann (McGill) for assistance with calcite cleavage and interpretation of XRD raw data. Bruno Lansard (McGill) for instruction on the use of the Alkalinity Titrator. Stelly Lefort (McGill) and Melissa Maisonneuve (McGill) for providing modified protocols for phosphate analysis and for demonstration. Varina Smith (McGill) for assistance with AFM. Dominique Richard (McGill) for her opinions, advice and extra pair of hands during high-frequency sampling for kinetic measurements.

Thais Lamana (McGill) for her opinions, discussion regarding PHREEQC and for lending a hand with phosphate analyses. Hao Bui (McGill) and André Pellerin (McGill) for access to and instruction on the stove-top autoclave. Bernardo Brixel (McGill), Qiang Chen (McGill), Crystal Mann (McGill), Tingting Wang (McGill) and Ruben Goethals (UvA) for their constructive criticism and reviews, penned and otherwise.

Staff Anne Kosowski (McGill), Kristy Thornton (McGill), Angela Di Ninno (McGill) and Brigitte Dionne (McGill) for administrative assistance throughout my residency in the MSc programme at McGill.

List of Figures

List of Tables

Chapter 1

Introduction & Objectives

This study addresses the role of microbial activity in the weathering of limestone. Weathering is literally defined as the breakdown of rock *in situ*[i] [1]. Therefore, it would follow that biologically-mediated weathering could be defined as the decomposition of rock mediated by biological activity, generally due to bacterial attachment and the creation of a microenvironment resulting from their activity and/or the release of metabolites at or near the solid surface. Our main focus was to identify the mechanism(s) by which bacteria modify calcium carbonate surfaces, metabolise the mineral constituents and alter the crystal surface in freshwater environments. In this study, we elected to focus on the modification of the most stable calcium carbonate polymorph, under earth surface conditions, calcite ($CaCO_3$), given its ubiquity in sedimentary environments and high reactivity. Essentially, this is a preliminary study focussed on determining calcite dissolution rates in the absence (abiotic) and presence of bacteria and identification of factors that induce bacterial attachment and colonisation of the mineral surface. Results of this study will provide critical information for conducting future experiments.

[i]Under earth surface conditions, when exposed to air, moisture and organic matter.

1.1 Context and Impetus

Connections between microbiology and geology have several ramifications. Bachofen (1991), Kasting (1993) and Kasting and Siefert (2002) are among the researchers who have demonstrated the important role of bacteria on earth surface evolution, including the uppermost lithosphere and the hydrosphere [2–6]. As a result of their findings, the role of bacteria in the formation of our current atmosphere is now better understood. Microbes can provide insights into elemental mobility and enable the application of such knowledge to environmental bioremediation [7]. Research has demonstrated that microorganisms are able to accelerate the release of elements from geologic materials [8][ii]. This may occur directly, in order to acquire nutrients necessary for biomass production (e.g. Welch *et al.* (2002)), or indirectly by excretion of metabolites that decrease pH, complex cations and/or change mineral saturation states of the solutions in which they bathe (e.g. Barker *et al.* (1998)) [9].

Friis *et al.* (2003) and L*ü*ttge and Conrad (2004) are among the few researchers [8, 10–13] who have investigated the effects of biological processes on calcite dissolution, in contrast to extensive reports on inorganic and biologically-mediated precipitation of calcite. These studies established that bacterial metabolism can influence pH, alkalinity and carbonate equilibria by releasing CO_2 and altering charge balance relationships during utilisation of carbon, nitrogen and other nutrients [8, 12, 14][iii]. These studies focussed on calcite dissolution in seawater and with model bacteria [8]. Even fewer studies have addressed how metabolising bacteria influence limestone weathering on the continents [8, 9]. In a recent paper, Jacobson and Wu (2009) report on an investigation of microbial interactions with calcite in the context of continental weathering, although as with previous studies, model bacteria were also employed. They established that the chosen model bacterial species is able to lower solution pH metabolically in the presence of glucose and ammonium, thereby accelerating calcite dissolution. We looked at the colonisation of calcite surfaces by a natural bacterial consortia. The experimental conditions closely reflected those occurring in nature.

[ii] And references therein

[iii] And references therein

1.2 Objectives

The main objective of the study is to determine whether bacterial attachment and metabolism can modify the dissolution kinetics and the surface of a calcite crystal in aqueous solutions. We first investigated the interaction between the microorganisms, the mineral and the aqueous solution under earth surface conditions (i.e. 25 °C (± 2 °C), 1 atm pressure). The research objective was addressed through a number of critical questions:

1. Is there preferential attachment of some bacterial species to limestone in nature?
2. Do they affect the calcite dissolution kinetics and surface?

The literature on the selective attachment of bacteria and their metabolic effects on mineral surfaces were reviewed extensively in Chapter 2. In this chapter, reports on bacterial strains that thrive on calcium carbonate are highlighted and the associated studies on how cultures of these bacteria affect calcite dissolution under controlled laboratory conditions.

1.3 Background

Calcite is the most common and most stable polymorph of calcium carbonate under earth surface conditions and is present in most natural aquatic systems. It is one of three $CaCO_3$ polymorphs, with aragonite and vaterite. Although aragonite is abundant in marine sediments and speleothems, it is metastable, and thus, calcite predominates due to its greater stability and the biological preference for its inclusion in exoskeletons. It is present in biogenic sediments as well as in sedimentary rocks. With the exception of dolomite ($CaMg(CO_3)_2$), calcite is virtually the only mineral present in limestone, a sedimentary rock which mostly forms by the accumulation and lithification of calcareous bivalves and microfossils (coccolithophores and foraminifera) [15, 16]. Calcite and dolomite are by far the most abundant carbonate minerals, comprising nearly 20% by volume of Phanerozoic sedimentary rocks [17].

1.3.1 Crystallography and Crystal Chemistry

Calcite has a trigonal crystal structure and three crystal habits namely prismatic, rhombohedral and scalenohedral. Iceland Spar calcite is one of several varieties of the mineral and was used in this study. It was originally discovered in Iceland and has rhombohedral cleavage. Calcite is an ionic mineral and its constituents, calcium and carbonate ions, are held together by electrostatic forces; each calcium atom is surrounded by six oxygen atoms. A true rhombohedral cell consists of eight small cells (each of which comprise four calcium carbonate units) and, thus, one rhombohedral true cell contains thirty-two calcium carbonate groups [15]. Calcite is easily cleaved; cleavage is perfect along faces of the morphological rhombohedron. The atomic planes parallel to cleavage faces are occupied by oppositely charged ions and, therefore, adjacent atomic planes parallel to the cleavage rhomb are held together by a juxtaposition of oppositely charged ions. The behaviour of calcite in aqueous environments is influenced strongly by its surface chemistry. The properties of the calcite surface will determine the type and rates of reactions that occur at the solid-water interface, including dissolution and precipitation reactions.

1.3.2 Calcite Weathering and Dissolution Kinetics

In natural systems, under physiological conditions (i.e. 1 atm pressure, 25 °C, pH 6-8, 0.085% saline), mineral weathering comprises reactions controlled by surface processes and transfer of reactants and products from the solid phase to the bulk solution [14]. There are two reaction mechanisms governing calcite/limestone weathering; transport (or diffusion) predominates at low pH, where dissolution occurs quickly and is only limited by the transport of reacting species from the mineral surface to the bulk solution [14]. At higher pH values, calcite dissolution rate is surface-controlled, where the rate of dissolution is limited by the chemical reactions occurring at the solid-liquid interface (*ibid*).

1.3.2.1 Dissolution Rate Equations

Calcite reaction kinetics has been the subject of extensive theoretical and experimental studies. Hence, several rate formulations have been proposed to fit or predict calcite dissolution (or precipitation) rates under a variety of chemical conditions [18]. In many cases, chemical reaction rates are expressed relative to the degree of disequilibrium (deviation from $\Delta G_{Rx} = 0$), at which the rate of the forward (dissolution) reaction is equal and opposite to that of the reverse (precipitation) reaction.

Whereas most ionic salts will dissociate into their constituent ions, carbonate ions liberated to solution upon carbonate mineral dissolution can participate, according to the pH of the solution, in a sequence of acid-base reactions which decrease its ion activity and increase the mineral solubility [19].

As with most weathering reactions, in addition to the minerals, water and carbonic acid (H_2CO_3) (acquired from the reaction of atmospheric or soil CO_2 with water) are the main reactants, where the latter acts as the proton-source. The reaction products usually include metal cations and a source of alkalinity, typically in form of bicarbonate (HCO_3^-). The reaction mechanism is usually complex and typically involves a suite of elementary, parallel or consecutive reactions [14].

There is no definitive description of the actual reaction mechanism of calcite dissolution in nature, as the process is influenced by several parameters of the carbonic acid system, including the degree of disequilibrium, and the influence of reaction inhibitors (e.g., phosphate) and catalyzers. Nevertheless, several have been proposed, based on classic chemical kinetics or surface complexation theory, to describe the dissolution process (see [18, 20–22].

In accordance with Wu and Jacobson (2009), calcite dissolution proceeds by three simultaneously-occurring parallel reactions, the predominance of which is dependent on pH, pCO_2 and mineral solubility [8]. These three reactions were originally proposed by Plummer *et al.* (1978) as

$$CaCO_3 + H^+ \longleftrightarrow Ca^{2+} + HCO_3^- \tag{1.1}$$

$$CaCO_3 + H_2CO_3^* \longleftrightarrow Ca^{2+} + 2HCO_3^- \tag{1.2}$$

$$CaCO_3 \longleftrightarrow Ca^{2+} + CO_3^{2-} \tag{1.3}$$

although the third was originally proposed as

$$CaCO_3 + H_2O \longleftrightarrow Ca^{2+} + HCO_3^- + OH^- \tag{1.4}$$

Chou *et al.* (1989) replaced the third reaction with reaction 1.3, adopted from a study by Reddy *et al.* (1981), altering the forward reaction mechanism. Plummer *et al.* (1978) established that reaction 1.1 prevails under acidic conditions, (where there is protonation of the crystal surface) and at low pCO_2, so the rate of dissolution is dependent on proton activity. Reaction 1.2[iv] predominates at intermediate pH and high pCO_2, where there is carbonation of the surface and thus, where the rate is dependent on the concentration of dissolved CO_2. Finally, reaction 1.4 dominates under high pH conditions. Under the latter conditions, the rate is constant (at high pH) and independent of the solution composition [20, 23]; it is transport-controlled and a function of stirring rate.

In accordance to these reactions, the overall forward (dissolution) reaction rate is expressed as

$$R = k_{1a_{H^+}} + k_{2a_{H_2CO_3^*}} + k_{3a_{H_2O}} \tag{1.5}$$

where R is the reaction rate, a_i are activities and k_1 to k_3 are dissolution rate constants for each of the three reactions described above, the values of which were evaluated by Plummer *et al.* (1978) and are temperature-dependent.

1.3.2.2 Surface Complexation

Calcite dissolution is complex and its rate is determined by the degree of disequilibrium, the solution composition (e.g., pH, pCO_2, Ca^{2+}:CO_3^{2-} ratio) as well as by the surface properties of the mineral-solution interface [24]. Several parameters, including specific surface area, cation exchange capacity, hydrophobicity and surface charge, define the nature of mineral surface reactions in aquatic environments (*ibid*).

Each mineral has its own characteristic surface charge, which is typically dependent on pH and the activity of other potential-determining ions [14, 25]. In the case of calcium carbonates, these include H^+, OH^-, Ca^{2+}, HCO_3^- and CO_3^{2-}. pH controls carbonate ion speciation and species predominance in solution (Figure 1.1) [25].

[iv] $H_2CO_3^* = H_2CO_3^0 + CO_2$

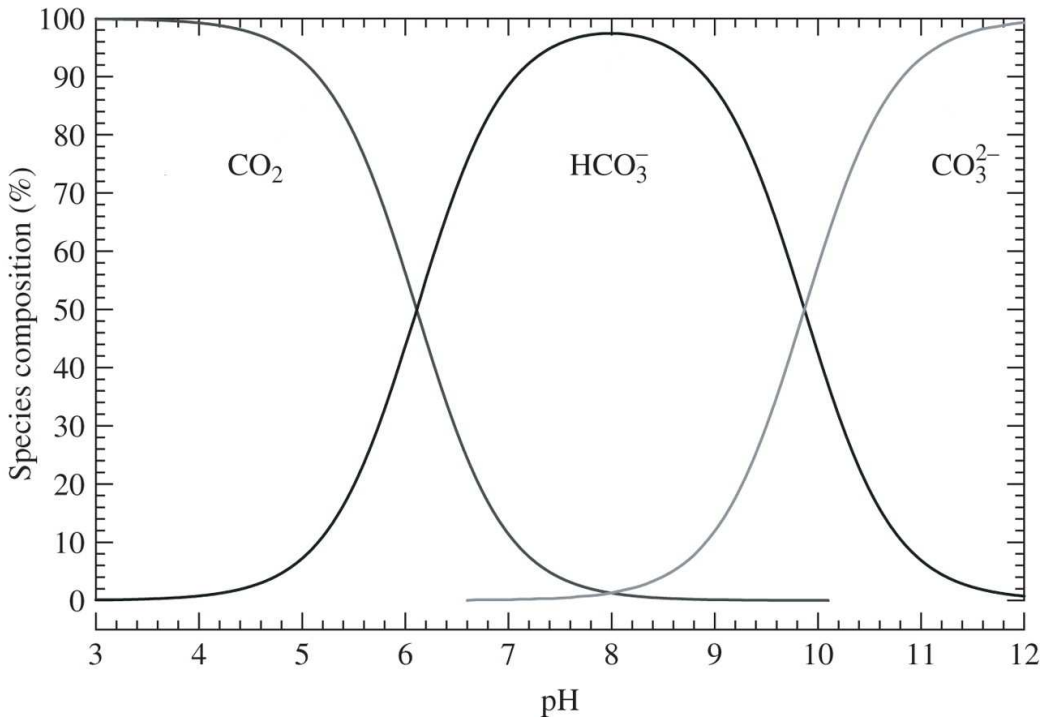

Figure 1.1: Carbonate species dominance in solution.

Hydrolysis processes and surface complexation determine the interfacial electrical properties of carbonate minerals [24], which in turn, affect calcite dissolution kinetics [22]. A mineral charge may develop as a result of structural substitutions and disorders from reactions with ionic species in aqueous solution [26]. There are three types of surface charge, the first of which is the structural charge (σ_0), which is due to lattice imperfections or isomorphous substitutions of atoms leading to a net charge. The second is the adsorbed proton charge (σ_H), due to acid-base chemical reactions at the mineral surface. The surface groups on a mineral surface can be protonated or de-protonated. The solution pH determines the extent of protonation; at low pH, the net surface charge will be positive and vice versa. Thirdly, surface charge can be modified by the adsorption of ions or hydrophobic species, including organic matter. This third form of surface charge is called the adsorbed ion charge, which can be positive (q_+) or negative (q_-) and is denoted as a net charge (δq) [14, 26].

Points of zero charge correspond to pHs at which two of the three types of charge are

equal to zero. These points vary with temperature, pressure and solution composition. The most notable point of zero charge is the point of zero net proton charge (pH_{pznpc}). This is the point at which $(\sigma_{H+}) = (\sigma_{OH-})$. The pH_{pznpc} for calcite is pH 9.5 [27]. The pH at which there is no net surface charge, is known as the point of zero charge or pH_{pzc} [26]. This point is more difficult to determine for calcite, as it varies with the solution composition, although it is estimated at pH 8.2 for 25 °C and atmospheric pCO_2 [18, 22].

The surface charge of minerals can normally be determined empirically. The structural charge and ion adsorption charges can be measured using adsorption methods while the proton charge is usually estimated by acid-base titrations of the surface [26], where a suspension of said mineral is titrated with an acid or base and the net uptake or release of protons or hydroxide ions by the mineral surface can be calculated via the pH and the amount of acid or base added to the suspension. However, most carbonate minerals, especially calcite, are too reactive for surface acid-base titrations since they readily dissolve or precipitate [22].

The surface chemistry of carbonate minerals in contact with water is described in terms of surface coordination reactions with the aqueous species: Ca^{2+}, CO_3^{2-}, HCO_3^-, $CaHCO_3^+$, H^+ and OH^- [24]. Van Cappellen *et al.* (1993) and Pokrovsky *et al.* (1999) devised surface-complexation models to illustrate the relationship between the dissolution kinetics of calcite and chemical speciation at the mineral-solution interface [22, 28]. The model assumes the presence of two main binding sites at the calcite surface: $\equiv CaOH^0$ and $\equiv CO_3H^0$, whose protonation/hydration and interactions with ligands control mineral reactivity in aqueous solutions [29]. As such, proton-promoted dissolution at low pH, as illustrated by reaction 1.1, is explained by the protonation of the carbonate site $\equiv CO_3H^0$, whereas the surface hydration reaction 1.4 is governed by the second site, $\equiv CaOH^0$ (*ibid*). The dissolution rate of calcite increases as carbonate surface sites are protonated and/or calcium sites are carbonated. These protonation and carbonation reactions generate increasingly reactive surface complexes, thereby enabling the release of surface cations to the bulk solution [22].

Bibliography

[1] B. W. Murck, B. J. Sinner, and S. C. Porter, *Environmental Geology*. New York: John Wiley & Sons. Inc, 1996.

[2] L. Wu, A. D. Jacobson, and M. Hausner, "Characterization of elemental release during microbe-granite interactions at T=28 °C," *Geochimica et Cosmochimica Acta*, vol. 72, no. 4, pp. 1076–1095, 2008.

[3] H. L. Ehrlich, "Geomicrobiology: its significance for geology," *Earth-Science Reviews*, vol. 45, no. 1-2, pp. 45–60, 1998.

[4] R. Bachofen, "Gas metabolism of microorganisms," *Experientia*, vol. 47, pp. 508–513, 1991.

[5] J. F. Kasting, "Earth's early atmosphere," *Science*, vol. 259, no. 5097, pp. 920–926, 1993.

[6] J. F. Kasting and J. L. Siefert, "Life and the evolution of earth's atmosphere," *Science*, vol. 296, no. 5570, pp. 1066–1068, 2002.

[7] L. A. Warren, "A special issue dedicated to microbial geochemistry," *Geochimica et Cosmochimica Acta*, vol. 68, no. 15, p. 3139, 2004.

[8] D. Jacobson, Andrew and L. Wu, "Microbial dissolution of calcite at T = 28 °C and ambient pCO_2," *Geochimica et Cosmochimica Acta*, vol. 73, pp. 2314–2331, 2009.

[9] L. Wu, A. D. Jacobson, H.-C. Chen, and M. Hausner, "Characterization of elemental release during microbe-basalt interactions at T= 28 °C," *Geochimica et Cosmochimica Acta*, vol. 71, no. 9, pp. 2224–2239, 2007.

[10] K. J. Davis, K. H. Nealson, and A. L*ü*ttge, "Calcite and dolomite dissolution rates in the context of microbe-mineral surface interactions," *Geobiology*, vol. 5, no. 2, pp. 191–205, 2007.

[11] A. K. Friis, T. A. Davis, M. M. Figueira, J. Paquette, and A. Mucci, "Influence of bacillus subtilis cell walls and EDTA on calcite dissolution rates and crystal surface

features," *Environmental Science and Technology*, vol. 37, no. 11, pp. 2376– 2382, 2003.

[12] A. Lüttge and P. G. Conrad, "Direct observation of microbial inhibition of calcite dissolution," *Applied and Environmental Microbiology*, vol. 70, no. 3, pp. 1627–1632, 2004.

[13] P. Bennett, F. Hiebert, and J. Rogers, "Microbial control of mineral-groundwater equilibria: macroscale to microscale," *Hydrogeology*, vol. 8, no. 1, pp. 47–62, 2000.

[14] W. Stumm and J. J. Morgan, *Aquatic Chemistry*. New York: John Wiley & Sons, Inc, 1996.

[15] F. Lippmann, *Sedimentary carbonate minerals*. Heidelberg: Springer-Verlag, 1973.

[16] C. Klein, *Manual of Mineral Science*. John Wiley & Sons, inc, 2002.

[17] J. W. Morse, R. S. Arvidson, and A. Lüttge, "Calcium carbonate formation and dissolution," *Chemical Reviews*, vol. 107, no. 2, pp. 342–381, 2007.

[18] T. Arakaki and A. Mucci, "A continuous and mechanistic representation of calcite reaction-controlled kinetics in dilute solutions at 25 °C and 1 atm total pressure," *Aquatic Geochemistry*, vol. 1, pp. 105–130, 1995.

[19] J. W. Morse and R. S. Arvidson, "The dissolution kinetics of major sedimentary carbonate minerals," *Earth-Science Reviews*, vol. 58, no. 1-2, pp. 51–84, 2002.

[20] L. N. Plummer, T. M. L. Wigley, and D. L. Parkhurst, "The kinetics of calcite dissolution in CO_2 -water systems at 5 degrees to 60 degrees c and 0.0 to 1.0 atm CO_2," *Am J Sci*, vol. 278, no. 2, pp. 179–216, 1978.

[21] L. Chou, R. M. Garrels, and R. Wollast, "Comparative study of the kinetics and mechanisms of dissolution of carbonate minerals," *Chemical Geology*, vol. 78, no. 3-4, pp. 269 – 282, 1989.

[22] P. V. Cappellen, L. Charlet, W. Stumm, and P. Wersin, "A surface complexation model of the carbonate mineral-aqueous solution interface," *Geochimica et Cosmochimica Acta*, vol. 57, no. 15, pp. 3505 – 3518, 1993.

[23] E. Busenberg and L. N. Plummer, "A comparative study of the dissolution and crystal growth mechanisms of calcite and aragonite," in *Studies in Diagenesis* (F. Mumpton, ed.), vol. 1578, pp. 139–168, U.S. Geological Survey, 1986.

[24] N. Vdović, "Electrokinetic behaviour of calcite–the relationship with other calcite properties," *Chemical Geology*, vol. 177, no. 3-4, pp. 241 – 248, 2001.

[25] S. L. S. Stipp, "Toward a conceptual model of the calcite surface: hydration, hydrolysis, and surface potential," *Geochimica et Cosmochimica Acta*, vol. 63, no. 19-20, pp. 3121 – 3131, 1999.

[26] G. Sposito, "On points of zero charge," *Environmental Science & Technology*, vol. 32, no. 19, pp. 2815–2819, 1998.

[27] H. Churchill, H. Teng, and R. M. Hazen, "Correlation of ph-dependent surface interaction forces to amino acid adsorption: Implications for the origin of life," *American Mineralogist*, vol. 89, no. 7, pp. 1048–1055, 2004.

[28] O. S. Pokrovsky and J. Schott, "Processes at the magnesium-bearing carbonates/solution interface. ii. kinetics and mechanism of magnesite dissolution," *Geochimica et Cosmochimica Acta*, vol. 63, no. 6, pp. 881–897, 1999. doi: DOI: 10.1016/S0016-7037(99)00013-7.

[29] O. S. Pokrovsky, S. V. Golubev, and J. Schott, "Dissolution kinetics of calcite, dolomite and magnesite at 25 °C and 0 to 50 atm pCO_2," *Chemical Geology*, vol. 217, no. 3-4, pp. 239 – 255, 2005.

Chapter 2

Influence of Bacteria on the Dissolution Rate of Minerals: A Literature Review

Sulu-Gambari, Fatimah[i*] and **Mucci,** Alfonso[i] and **Frigon,** Dominic[ii]

2.1 Abstract

Microbes that contribute to rock weathering often grow on rock surfaces as biofilms. Bacteria attach to surfaces biologically, through specific interactions, or physicochemically, through non-specific interactions. A wide range of surface components, collectively known as adhesins, have been implicated in specific attachment. Non-specific attachment is dependent on the properties of the bacteria-mineral and bacteria-solution interfaces and, thus, depends on surface properties including cell surface hydrophobicity and electrokinetic potential. Microbial-facilitated dissolution of

[i]Earth and Planetary Sciences, McGill University, Montréal
[*]Corresponding author: ✉ fatimah.sulu-gambari@mail.mcgill.ca
[ii]Civil Engineering, McGill University, Montréal

mineral surfaces may occur directly, where there is likely contact-mediated catalysis of the dissolution process in order to acquire nutrients necessary for biomass production. Alternatively, dissolution may be induced indirectly, where metabolites are excreted by microbes. These metabolites, including ligands and acids, decrease pH, complex cations and/or modify the saturation state of the bulk or local solution with respect to the colonised mineral.

keywords bacteria, surface recognition, attachment, biofilm, inorganic acids, organic acids, organic ligands

2.2 Introduction

There is a limited amount of literature that addresses the bacterial attachment to and subsequent dissolution of mineral surfaces. Most studies have focussed on the precipitation of biotic minerals [1]. Consequently, this review includes reports on the microbial dissolution of mineral surfaces in general, rather than a specific mineral class. It also includes reports of bacterial attachment to synthetic surfaces in the discussion of relevant mechanisms and/or processes.

2.3 Proposed Mechanisms of Microbe-mediated Dissolution

Microbe-mediated weathering is a process best divided into three steps. The first is the recognition and subsequent attachment of bacteria to a given surface. The second is colonisation. The final stage is the induction of dissolution of the mineral surface. These steps are discussed separately:

2.3.1 Surface Recognition and Attachment

2.3.1.1 Recognition

The assumption is that bacteria are capable of 'recognising' surfaces to which they attach. The term recognition implies a specific microbial affinity for a given mineral surface relative to others and is gauged in terms of the number of attached cells. The principles of surface recognition are presented by Busscher and Weerkamp [2] as the 'specific receptor' concept, involving stereochemical molecular interactions between cell wall components and substrates. Molecular interactions may be defined as those (microscopic) that take place between stereochemically complementary surface components over extremely short distances (< 1.5nm). This enables specific ionic, hydrogen and possibly chemical bonding, as opposed to non-specific interactions, which may modify the overall (macroscopic) surface properties of the mineral, including charge or surface free energy (*ibid*). An elaboration follows in the next section.

Multiple recognition studies have been carried out on minerals such as silicates (e.g. [3]), oxides (e.g. [3–5]), sulphides ([6–8]) and carbonates (e.g. [1, 3, 9]). Lower *et al.* [3] and L*ü*ttge and Conrad [9] investigated the microbial surface-recognition of calcite, using the same bacterial strain. The former group concluded that *Shewanella oneidensis* MR-1 is capable of recognising silicate and oxide mineral surfaces, whereas the latter group of researchers found that these bacteria not only recognise calcite surfaces but also recognise specific high energy sites at the surface [9].

2.3.1.2 Attachment

Bacteria attach to a surface biologically, through specific interactions (via cell-surface appendages), or physicochemically through non-specific interactions (via long-range and short-range attraction between microbes and a substrate). Active bacteria are capable of attaching to almost any surface, subsequently multiplying and aggregating for ecological reasons including survival and dispersal [10]. Biofilm formation appears early in geologic history, as evident from the fossil record (3.25 Ga stromatolites). It is apparently a critical factor for bacterial survival in diverse environments [10].

In general, with regards to specific molecular interactions between microbes and

minerals, a wide range of surface components can be found that have been implicated in adhesion. Several of these are molecular probes that react stereochemically with molecules on substrate surfaces and are described as *adhesins* [2, 11]. The presence of *adhesins* on a bacterial cell surface determines the surface characteristics of the cell and, thereby, its overall adhesion properties. The influence of appendages on adhesion is largely dependent upon their abundance and on topographic distribution [11].

The main types of polymers found at the bacterial cell surface are proteins and polysaccharides or a combination of both [12]. The amount of polymers produced is species- and age-dependent and is also determined by growth conditions. The appendages differ in shape, size and structure [13]. Their composition determines the type and strength of bonding and the number of possible bonding sites (*ibid*). Polymers of lower molecular weight adsorb in compact conformation and, thus, more weakly than larger appendages [11, 13]. Structure and shape depend on the orientation of the polymer functional groups, whether they are linear, branched, or cross-linked. Additionally, the appendages themselves may be coiled or uncoiled [13]. Both gram-positive and gram-negative bacteria[iii] have been shown to possess a range of surface layers and appendages of differing structural and chemical nature, with differing physicochemical properties [2].

Bacterial attachment is also dependent on the properties of the bacteria-mineral and bacteria-solution interfaces. The surface properties of bacteria that affect adhesion include cell surface hydrophobicity and electrokinetic potential [14]. It is important to note that these surface characteristics are influenced by the properties of surface appendages (i.e. hydrophobicity, charge and surface free energy) [2].

Under physiological conditions (i.e. 1 atm pressure, 25 °C, pH 6-8, 0.085% saline), biological surfaces carry a net negative charge, mainly due to the presence of de-protonated carboxyl and phosphate groups [2, 15]. In gram-positive bacteria, teichoic and teichuronic acids of the cell wall, as well as acidic polypeptides and polysaccharides of the glycocalyx[iv], are believed to contribute to the negative charge. In gram-negative

[iii] Bacteria are classified in two categories based on their cell-wall structure. Gram-positive bacteria cell walls consist of a thicker peptidoglycan layer than the walls of gram-negative bacteria

[iv] The outer component of a bacterial cell

bacteria, acidic lipopolysaccharides and proteins of the outer cell membrane, in addition to extracellular polymers of the glycocalyx, are all sources of negative charge. The surface free energy of bacterial cells[v] is variable as some bacteria are relatively hydrophobic and others more hydrophilic. Since the distribution of hydrophobic sites on crystals are not usually uniform, some bacteria are seen to display preferred orientations at interfaces [16].

Surface free energy is only one of the main physicochemical factors that influence attachment. Another, more prominent factor, is the presence of interfacial forces, namely Derjaguin Landau and Verwey Overbeek (DLVO)[vi] energies, named for a theory (of the same name) that describes the adhesion of interacting colloids and that introduces several principles developed to explain physicochemical adhesion of microbes to substrates. Bacteria are in the same size range as colloidal particles and, therefore, their interfacial interactions (with surfaces) are often regarded as analogues in adhesion studies on microbe-mineral interactions [5, 11, 17–19]. Model bacteria, cultured in the laboratory and employed in these studies, unlike wild-types, are unable to express[vii] the cell-surface appendages that would be important for survival in a hostile 'wild' environment. These surface structures are necessary for biological interactions and, therefore, model strains are similar to smooth-surfaced colloids [19]. Hence, their adhesion is best explained from a physicochemical viewpoint [11].

DLVO forces comprise short-range van der Waals interactions and long-range electrostatic forces. For all intensive purposes, the energies/forces are of interest here, though the theory itself is beyond the scope of this study and has been described as inconclusive. This is mainly because, unlike colloidal particles, natural bacteria are not smooth-surfaced and the interactions of these cells with substrate surfaces, mineral or otherwise, occurs primarily by bridging of bacterial fibres with complementary

[v]The excess energy per unit area due to the presence of an interacting surface. It is the superfluous bonding potential that would otherwise be used to increase the bacterial cell surface area by unit area i.e. by binding to a substrate

[vi]Derjaguin & Landau and Verwey & Overbeek are two groups of scientists who, independently, investigated the attractive forces between colloidal particles and arrived at the same conclusions.

[vii]i.e. synthesise

appendages on the substrate. In addition, the DLVO theory makes certain assumptions, including that surface properties, such as surface charge, are uniform on the surface of the substrate, yet, as discussed above, wild bacteria are seen to attach at certain sites of higher energy or of particular hydrophobicity. Thus, there are several discrepancies between the DLVO model for colloids and the empirical observations of bacterial adhesion to surfaces. In fact, most laboratory studies show increased bacterial adhesion/aggregation in comparison to the model[viii]. Hence, the DLVO theory is of limited application in the study of bacterial adhesion [19].

As bacterial surfaces are mainly negatively charged under physiological conditions, they attract positive counterions from the surrounding aqueous environment. These ions form a layer described as an electrical double layer (EDL)[ix]. The EDL is also divided in two: the Stern layer, where the ions closest to the surface or the cell wall are bound strongly, and the diffuse layer, the outermost section of the EDL made up of mobile ions held more loosely through long-range electrostatic interactions.

Far apart (> 50nm), van der Waals forces of attraction predominate, bringing particles towards each other. At shorter distances (10-20nm), the EDLs begin to overlap and electrostatic repulsion prevails. This repulsive electrostatic force creates a barrier that is known as a 'secondary minimum', which, when overcome, allows the particles to move closer together. At this secondary minimum, the particles are loosely held together, moving independently, displaying Brownian motion and can readily be separated by a small perturbation of the system. This is reversible adhesion. When the particles are closer to each other, they attract each other via van der Waals forces. Once the 'secondary minimum' is overcome, or at a given distance from each other (< 1.5nm), the attractive forces between two particles are much stronger than the counteracting repulsive forces and can hold the particles together.

When the two component forces are added, the net force determines the extent of adhesion between the particles. If the particles possess enough kinetic energy, they will overcome a 'primary minimum', which is a second energy barrier, at which point they will be in such great proximity that attractive van der Waals forces as well as other short-range interactions including dipole interactions, covalent bonding and the

[viii] The difference is attributed to the presence of bacterial appendages.

[ix] This is also a model theory.

aforementioned hydrophobic interactions, will bind the particles irreversibly (Figure 2.1) [2, 12]. As mentioned earlier, there are numerous factors that influence the adhesion of bacteria to surfaces (mineral or otherwise) in aqueous solutions. These are dependent on both the nature of the bacterial cells as well as the surface properties of the substrate. Generally, and not in keeping with colloidal theory, wild bacteria will adhere equally well to very hydrophobic and very hydrophilic surfaces, smooth or rough surfaces in high or low-shear flow systems [19].

2.3.2 Biofilm Formation

Microbes, not limited to bacteria but including algae, fungi and lichens that contribute to rock weathering, often grow on rock surfaces in the form of biofilms. Microbial biofilms can be described as ecosystems of interacting bacterial communities[x] with high population densities that associate with surfaces; they are structurally complex and dynamic systems [10, 20]. They can also be distinguished from their planktonic counterparts by the presence of an extracellular polymer substance[xi] (EPS) matrix, which is the main component of all biofilms [20]. It is the EPS that determines the physical properties of a biofilm and the constituent bacteria determine the physiological properties of the ecosystem. The EPS is linked to processes and properties integral to behaviour including attachment, detachment (to and from surfaces), mechanical strength and antibiotic resistance [10, 20, 21]. Bacterial attachment is influenced by EPS production as the polysaccharides ensure irreversible attachment of cells to the surface. The efficiency of adhesion of the microbes to a given substrate may also influence biofilm growth.

Biofilm formation depends on a number of physical and environmental conditions including the morphology of the substrate that will serve for anchorage, interfacial characteristics such as hydrophobicity or surface charge, and the solution chemistry (i.e. pH and ionic strength) [22].

All biofilms, regardless of structure or function, develop in a three-step process. Biofilm growth begins with the adsorption of a conditioning film of organic matter. This process

[x] Bacterial biofilms may also include other microbial organisms.

[xi] or extrapolymeric substances

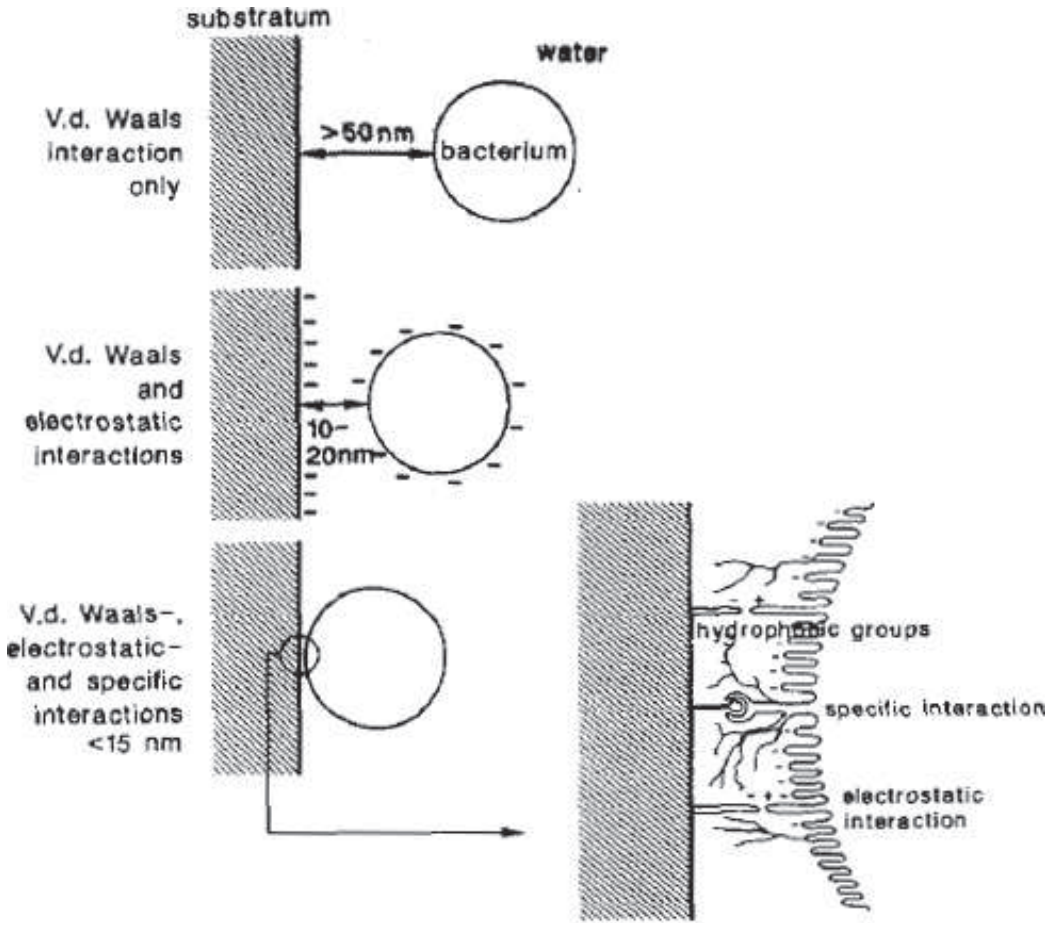

Figure 2.1: Stages of bacterial adhesion to solid surfaces. At large distances (> 50nm), only attractive van der Waals interactions are effective. The separation distance is too large for the interacting surfaces to recognise specific surface components. At distances between 10 and 20nm, 'secondary minimum' interactions occur due to electrostatic repulsion. Adhesion at this stage is reversible. At short separation distances (< 1.5nm), where the potential energy barrier has been overcome, specific interactions, including short-range polar forces, can occur. These will lead to irreversible bonding [2].

occurs before any bacteria present in the system will adhere, simply because transport and adsorption of organic molecules are faster. Subsequent adhesion of microorganisms will occur. This step is initially reversible, as the microorganisms are only weakly bonded to the surface [21]. At the third stage of colonisation, excretion of EPS, as bacterial metabolites are produced, anchors the bacteria to the substrate and to each other, at which point adhesion becomes irreversible [21, 23]. Thereafter, the microorganisms continue to grow and multiply.

In addition to normal cell growth, biofilms produce large amounts of EPS. EPS is highly hydrated, as it incorporates a large amount of water via hydrogen bonding, and prevents desiccation [20, 23]. EPS typically comprises between 50 and 90% of the total organic carbon contained in a biofilm. Depending on the strain, growth conditions and age, biofilm thickness can range from a few micrometres to a centimetre [20]. The amount of EPS produced, the specific composition and chemical reactivity is also age-, species- and nutrient-dependent, where an excess in available carbon and limitation of nitrogen, potassium or phosphate are reported to promote its synthesis [23].

2.3.3 Microbe-Mineral Dissolution

Various types of bacteria have been used in dissolution studies. See Table 2.2 on page 30 for a summary. In most dissolution experiments, the choice of bacterial strains depended on the type of the rock/mineral to which they adhered. Bacteria excrete metabolites that alter the chemistry of the mineral (or the solution at the) surface, prompting dissolution [21, 24].

Most discussions involving the likelihood and efficiency of bacterial attachment to mineral surfaces and biologically-induced dissolution, though geared toward all mineral types, are based on literature which mainly pertains to silicates. This is expected as silicates are the most abundant minerals on the earth's surface and mantle and are, thus, the most investigated minerals with regards to weathering (e.g. [24–27]). Investigation of carbonate dissolution, as with silicates, is normally related to studies on the weathering processes.

Literature to-date reveals that microbial-facilitated dissolution of mineral surfaces may occur directly or indirectly [21, 24]. In the former case, there is likely contact-mediated

catalysis of the dissolution process upon attachment, most probably in order to acquire nutrients necessary for biomass production. In the latter case, it is attributed to dissolution by metabolites (EPS and non-EPS) excreted by microbes that decrease pH, complex cations and/or modify the saturation state of the bulk or local solution with respect to the colonised mineral [9, 24, 28].

2.3.3.1 Non-EPS Metabolites

Microbes can excrete chemical agents including mucopolysaccharides, ligands and acids, both organic and inorganic, that can locally accelerate mineral weathering [21, 24].

- Some microbes excrete inorganic acids, including weak acids such as carbonic acid (H_2CO_3), formed from the reaction of water with CO_2 as a product of respiration, or strong acids including nitric acid (HNO_3) and sulphuric acid (H_2SO_4) that promote the corrosion of rock material [21, 29, 30]. This would be an indirect dissolution mechanism.
- Soluble low-molecular-weight ($M_r < 1000$) organic acids, also excreted by bacteria, are able to act as acidulants, indirectly accelerating aluminosilicate mineral dissolution [31, 32]. Although most organic acids are weak acids, they increase mineral weathering through protonation of the surface [21]. Organic acids that are commonly produced by soil bacteria and, thus, relevant to the weathering process include 2-ketogluconic, lactic, acetic, citric, oxalic, pyruvic and succinic acids [21, 24].
- Organic ligands are thought to directly attack mineral surfaces by complexing with ions at the surface, pulling cations from the crystal lattice framework, weakening metal-oxygen bonds, facilitating breakage of framework bonds and catalysing dissolution reactions [13, 21, 31]. One proposed mechanism involves inner-sphere adsorption of the ligand, weakening critical lattice bonds at the adsorption site due to inductive effects including charge transfer [33, 34].

  Alternatively, ligands may work indirectly, by complexing ions in solution and decreasing its saturation state with respect to the mineral under investigation [21, 35]. Welch and Ullman [36] report that proton-promoted dissolution becomes

relatively more important at acidic pHs but that ligand-promoted dissolution dominates at near-neutral pH, where free protons are less abundant and, thus, proton-promoted dissolution (i.e. surface protonation) is relatively slow [30, 36]. Ullman *et al.* [32] reported that the impact of organic acids on the rate of silicate mineral dissolution is dependent on the ligand and on its concentration, on the pH of the solution and the composition of the mineral under study (feldspar) (*ibid*). Their experiments also revealed that polyfunctional (e.g. oxalate, succinate) organic ligands enhance dissolution rates more significantly than their monofunctional counterparts (e.g. acetate) (*ibid*).

- Siderophores, which are described as Fe(III)-specific bidentate ligands, also increase mineral dissolution on excretion by bacteria [25]. Siderophores are produced by aerobic and facultative-anaerobic bacteria under low iron conditions [21, 37]. They are soluble compounds of relatively low molecular weight ($M_r < 1500$) that have a high affinity for Fe(III). They comprise two classes, namely hydroxamates and catechols, both of which form bidentate 5-member chelates with the ion at mineral surfaces. This is thus a direct mechanism of dissolution [21].

  Bacteria can scavenge the Fe in iron oxides such as goethite (FeO(OH)) or iron silicates including olivine ($(Mg,Fe)_2SiO_4$) and biotite ($K(Mg,Fe)_3Al\ Si_3O_{10}(F,OH)_2$), which influences their rate of weathering. As these minerals are not readily soluble at near-neutral pH conditions, bacteria secrete siderophores that increase the Fe(III) concentration in solution to concentrations suitable for use in metabolism. The siderophore complexes with Fe(III) and the entire complex is taken up by the cell. Reduction takes place within the cell, converting Fe(III) to Fe(II) [26].

- Bacteria produce enzymes to degrade substrates such as cellulose that have crystalline structures similar to those of silicate minerals. It is also debated whether bacteria produce similar enzymes to aid the breakdown of mineral surfaces to liberate elements necessary for metabolism. The excretion of 'mineralases' has not been investigated [21].

The nature of reactions between organic acids and functional groups exuded by microbes at the solid-liquid interface is an integral part of determining the kinetics of

microbe-induced dissolution of given minerals. The mechanisms are still poorly understood [38].

2.3.3.2 Microenvironments

The excretion of chemical agents, as a result of microbial metabolism, produces a microenvironment whose chemistry differs from that of the bulk solution with which it has restricted exchange [32].

The microenvironment differs from the bulk solution in terms of pH, dissolved oxygen and organic/inorganic species concentrations [39]. The modified chemistry may facilitate the dissolution of the substrate surfaceThis facilitation is known as indirect dissolution. Microenvironments have characteristically low pH that can typically promote dissolution [40], although the exact chemistry of a given environment is species- and mineral-specific and would depend on the chemical agent(s) being exuded. Microzonations can be studied using microsensors, which are needle-shaped microelectrodes and are sensitive to pH and to specific compounds like oxygen, sulphide and nitrate [41, 42]. Microelectrodes have been used to study oxygen respiration, sulphide reduction and oxidation, as well as photosynthesis in biofilm microenvironments at spatial resolutions of less than 100μm [41–43][xii].

2.4 Previous Dissolution Studies

Microbially-induced dissolution has been mostly investigated with silicates, but also with phosphates, oxides and oxyhydroxides and more recently, with carbonates. A literature-review of these studies follows. See Tables 2.1 and 2.2 on pages 29 and 30 for a summary of the experimental observations and conclusions.

[xii] and references therein

2.4.1 Silicates

Buss *et al.* (2007) investigated the effects of siderophore-promoted dissolution of iron silicates ($Ca_2(Mg,Fe,Al)_5(Al,Si)_8O_{22}(OH)_2$) (hornblende). Enhanced dissolution as evidenced by biopitting was reported. They isolated *Bacillus sp.*, an obligately aerobic soil bacterium from a horneblende-containing soil from Gore Mountain, New York. It was chosen because it grows vigorously and produces siderophores in iron-deficient growth media in the presence of hornblende or hornblende glass [25].

Liermann *et al.* (2000) isolated *Streptomycete sp.* from hornblende-rich Adirondack soil collected at Gore Mountain in the Adirondack range, New York. Hornblende is described as a 'garbage mineral', as it is a common source of limiting trace metals required by bacteria for structure and function of enzymes, co-enzymes and co-factors. *Streptomyces* are known to release a Fe(III)-specific siderophore that enhances hornblende dissolution, through formation of pH microenvironments [26].

Barker *et al.* (1998) obtained lab cultures of five naturally-occurring subsurface bacterial strains for their experiments while investigating the effects of bacteria on aluminosilicate weathering. They were selected for their ability to produce organic acids and extracellular polymers that induce dissolution [24]. Of the five strains, the taxonomy of two were established in the study, one gram-positive strain belonging to the *Arthrobacter* genus of soil- dwelling microbes and another observed as closely related to *Burckholderia solanacearum*. *Burckholderia* is a genus comprising mainly of gram-negative, obligately aerobic pathogenic[xiii] microbes. These, in addition to two other strains, were isolated from the Middendorf formation at the Savannah River in South Carolina. The last strain was isolated from the PeeDee formation (*ibid*). No description of the environment of the sample site was provided i.e. whether from a soil, regolith, groundwater or other aquatic setting. The production of inorganic and organic acids by the bacteria was reported, resulting in a subsequent release of cations into solution.

Vandevivere *et al.* (1994) employed subsurface bacteria isolated from the PeeDee formation, the Middendorf formation and the Black Creek formation for their

[xiii] Including plant, human and animal pathogens

earlier study on the enhancement of bytownite ($(Ca,Na)(Si,Al)_4O_8$) dissolution at near-neutral pH. Indirect dissolution by a subsurface microbe identified as *Pseudomonas sp.* was reported. Bytownite, a calcium-rich feldspar, was selected as feldspars are among the most abundant rock-forming minerals in the crust and because calcium-rich feldspars dissolve more rapidly than others, allowing for short, practical experiments [27].

Ullman *et al.* (1996) provided in vitro evidence of the bacterial mediation of silicate dissolution in subsurface continental environments. Experiments were conducted on feldspars and quartz (SiO_2) and unnamed model bacteria were obtained from the subsurface microbial culture collection (SMCC)[xiv] at Florida State University laboratories and commercial sources [32].

Santelli *et al.* (2001) reported the inhibitory effect of iron-oxidisers on the dissolution of iron-containing silicate minerals. The chosen mineral was fayalite (Fe_2SiO_4) and the bacterium was *Thiobacillus ferrooxidans*, a lithotrophic iron-oxidising microbe, though its origin was not mentioned [44].

2.4.2 Oxides and Oxyhydroxides

Arnold *et al.* (1998) reported the enhanced reductive dissolution of goethite by *Pseudomonas sp.* 200. It is said to be one of the several bacterial classes that catalises this process; the other types include *Thiobacillus thiooxidans*, *T. ferrooxidans*, *Bacillus circulans*, *Bacillus polymyxa*, *Clostridium butyricum*, *Vibrio sp.* and *Sulfolobus acidocaldarius* [45]. The researchers explain that dissimilatory iron reduction involves the direct transfer of electrons from enzymes of the electric transport chain to Fe(III) (*ibid*). The bacterium was isolated 8 years prior from the Edmonton terminus of the Pembina oilfield pipeline, whose iron-reducing capabilities contributed to accelerated pipeline corrosion [45–47].

Hersman *et al.* (1995) also looked at metal oxide dissolution by soil bacteria, *Pseudomonas sp.* siderophores. The group investigated the effects on haematite (Fe_2O_3)

[xiv] US Department of Energy

[37], reporting siderophore-promoted dissolution at low pH, though the source of the bacteria was undisclosed.

Lüttge *et al.* (2005) describe investigations by Lower *et al.* [4, 5] on *Shewanella oneidensis* MR 1, a gram-negative anaerobic bacterium found in soils, sediments, surface and ground waters, involved in dissimilatory Fe(III) reduction. This research group reported the recognition by these microbes of goethite and diaspore surfaces. The origin of the bacteria used in this study was undisclosed, but the same bacterium was used in a subsequent study by Lower [5] and it is mentioned to have been obtained from the American Type Culture Collection in Manassas, Virginia [9].

Grantham *et al.* (1997) also looked at the catalytic dissolution of iron and aluminium oxyhydroxides by the model bacterium *S. oneidensis* MR 1, then called *Shewanella putrefaciens*. The oxyhydroxides used in this study were applied as a surface coating to quartz and silica glass rather than naturally-occurring metal oxyhydroxide minerals. As with the *Pseudomonas sp.* used in the previously discussed study by Arnold *et al.* [45] and to which *S. putrefaciens* bears phylogenetic relation, this microbe was isolated from the Pembina pipeline. They report that *S. putrefaciens* has since been isolated from diverse aquatic environments and is considered one of the most efficient and versatile dissimilatory metal-reducing microbes. They also note that the bacterium is able to reduce various redox species (e.g. Fe(III), Mn(IV)), which often occur as oxyhydroxide coatings on mineral surfaces in natural porous media systems [48].

2.4.3 Phosphates

Welch *et al.* (2002) reported enhanced dissolution of apatite ($Ca_5(PO_4)_3(F,Cl,OH)$) crystals in naturally-weathered granite. The increased dissolution rate resulted from microbial organic acid production in the presence of wild bacteria. The microbes were isolated from the Bemboka Granite, New South Wales, although it is not indicated whether these are bacteria, archea, fungi or a combination [35] .

2.4.4 Sulphides

Members of the bacterial genera *Sulfobacillus*, *Leptospirilum*, *Acidimicrobium* and *Thiominas* are among several classes of microbes (not restricted to bacteria) known to contribute to sulphide dissolution [49].

Jia *et al.* (2008) reported the selective adhesion of bacteria to sulphide mineral surfaces, on pyrite, galena (PbS) and sphalerite ((Zn,Fe)S) samples collected from a lead-zinc mine in north-eastern China. They obtained the three bacterial strains from the Institute of Microbiology at the Chinese Academy of Science (CAS): *Gordonia amarae*, *Mycobacterium phlei* and *Bacillus mucilayinosus* [50].

2.4.5 Carbonates

Investigation of carbonate dissolution, as with silicates, is normally related to studies on the biological influence of weathering processes. Most studies focussed on the biogenic dissolution of calcite and dolomite.

Davis *et al.* (2007) reported the enhanced dissolution of calcite and dolomite by *S. oneidensis* MR 1, a bacterium described above, which is normally involved in dissimilatory iron and manganese reduction. They chose this bacterium based on the results of a study of calcite dissolution by L*ü*ttge and Conrad [1]. The latter group of researchers selected this strain because it is known to attach to many substrates of no metabolic significance and because its attachment to carbonates had not previously been studied. The natural culture was isolated from Oneida Lake in New York State and is a member of a microbial group that is common in aquatic environments. They attach rapidly to mineral surfaces and are known as 'interface organisms' based on their propensity to be found at redox interfaces in natural systems (*ibid*).

Friis *et al.* (2003) studied the dissolution of calcite in the presence of inactive *Bacillus subtilis* a common, gram-positive soil bacterium. This type of bacterium was chosen on the basis of the molecular construction of the cell membranes and specifically,

the presence of functional groups including carboxyl and phosphate groups. The culture was obtained from the University of Guleph, but the nature of the culture (i.e. natural or model bacteria) was unspecified [51]. No significant effect of the cells on dissolution was reported.

Jacobson and Wu (2009) conducted dissolution experiments on calcite using *Burkholderia fungorum*, a rod-shaped gram-negative bacterium, available from the American Type Culture Collection[xv], they reported enhanced dissolution in biotic experiments. This bacterium is commonly associated with basalt and granite. It was adopted from their previous studies on those two rock types, based on the research group's familiarity with the physiology and growth characteristics of the microorganism [28, 52, 53].

2.5 Conclusion

Several strains of bacteria have been used in dissolution studies depending on the type of the rock/mineral to which they adhere in nature. Most of the studies discussed here made use of model bacteria. However, lab-adapted strains lack many surface structures (that would be necessary for survival in a hostile 'wild' environment) and are therefore similar to the smooth-surface colloidal structures visualised in the DLVO theory [19]. Natural bacteria are not smooth-surfaced and the interaction of these cells with surfaces is based on the bridging of bacterial fibres with complementary appendages on the surface being adhered to. Hence, the DLVO theory is of limited application to the study of bacterial adhesion (*ibid*). Bacteria will attach to any surface biologically (via cell-surface appendages), or physicochemically (via long-range and short-range forces).

Microbes are able to accelerate the release of elements from geologic materials, whether it is to acquire nutrients necessary for biomass production or by excretion of metabolites that alter the chemistry of the solutions in which they bathe [24, 35]. They can excrete chemical agents including mucopolysaccharides, ligands and acids, both organic and inorganic such as carbon dioxide, sulphuric and nitric acids that can locally accelerate

[xv] As with L*ü*ttge *et al* (2005)., see section on oxides and oxyhydroxides above

Table 2.1: Bacteria used in selected studies

Mineral Class	**Research Group**	**Mineral**	**Microbe**	**Study**
Silicates	Buss, Lüttge & Bentley., 2007	hornblende	*Bacillus sp.*	Dissolution
	Liermann *et al.*, 2000	hornblende	*Streptomycete*	Dissolution
	Barker *et al.*, 1998	aluminosilicates	*Anthrobacter* and *Burckholderia solanacearum*	Dissolution
	Vandevivere *et al.*, 1994	bytownite	*Pseudomonas sp.*	Dissolution
	Ullman *et al.*, 1994	silicates (feldspars & quartz)	unnamed	Dissolution
	Santelli *et al.*, 2001	fayalite	*Thiobacillus ferrooxidans*	Dissolution
Oxides & Oxyhydroxides	Arnold *et al.*, 1988	goethite	*Pseudomonas sp. 200*	Dissolution
	Hersman *et al.*, 1995	haematite	*Pseudomonas sp.*	Dissolution
	Grantham *et al.*, 1997	metal oxyhydroxides	*Shewanella oneidensis* MR 1 (formerly known as *Shewanella putrefaciens*)	Dissolution
	Lower *et al.*, 2001	goethite & diaspore	*Shewanella oneidensis* MR 1	Surface recognition
	Lower *et al.*, 2005	goethite	*E. coli* & *Shewanella oneidensis* MR 1	Surface recognition
Phosphates	Welch *et al.*, 2002	biotite & apatite crystals in weathered granite	unnamed	Dissolution
Sulphides	Jia *et al.*, 2008	pyrite, galena & shalerite	*Gordona amarae*, *Mycobacterium phlei* & *Bacillus mucilayinosus*	Adsorption
Carbonates	Davis *et al.*, 2007	calcite & dolomite	*Shewanella oneidensis* MR 1	Dissolution
	Friis *et al.*, 2003	calcite	*Bacillus subtilis*	Dissolution
	Jacobson & Wu, 2009	calcite	*Burholderia fungorum*	Dissolution

Table 2.2: Selected relevant microbe-induced dissolution studies

Mineral Class	**Research Group**	**Mineral**	**Observation**
Silicates	Buss, Lüttge & Bentley., 2007	hornblende	Enhanced dissolution in the presence of siderophores → evidence of biopitting
	Liermann *et al.*, 2000	hornblende	Formation of pH microenvironments
	Barker *et al.*, 1998	aluminosilicates	Bacterial production of inorganic and organic acids → increased release of cations into solution
	Vandevivere *et al.*, 1994	bytownite	Enhanced dissolution at near-neutral pH → no contact between bacteria and surface required
	Ullman *et al.*, 1994	silicates (feldspars & quartz)	Bacterial production of organic acids in organic-rich/ nutrient-poor cultures → enhanced mineral dissolution compared to controls
	Santelli *et al.*, 2001	fayalite	Inhibited dissolution → accumulation of Fe (III) on mineral surface sites
Oxides & Oxyhydroxides	Arnold *et al.*, 1988	goethite	Enhanced reductive dissolution → contact required for dissolution
	Hersman *et al.*, 1995	haematite	Siderophore-promoted dissolution at low pH
	Grantham *et al.*, 1997	metal oxyhydroxides	Localised pitting corresponding directly to sites of bacterial surface adhesion
Phosphates	Welch *et al.*, 2002	biotite & apatite crystals in weathered granite	Bacterial organic acid production → reduced pH → enhanced dissolution
Carbonates	Davis *et al.*, 2007	calcite & dolomite	Enhanced dissolution in early stages of bacterial colonisation
	Friis *et al.*, 2003	calcite	No significant increase in dissolution rates compared to abiotic controls
	Jacobson & Wu, 2009	calcite	Enhanced dissolution relative to abiotic controls

mineral weathering [30]. The excretion of these chemical agents, as a result of microbial metabolism, produces a microenvironment whose chemistry differs from that of the bulk solution with regards to pH and dissolved oxygen among other parameters. The chemistry of these microenvironments facilitates the dissolution of the substrate surface. Microenvironment formation is dependent on the rocks' physicochemical features and the interactions with the biofilm. Microenvironments have characteristically low pH that can promote dissolution [40]. The type of surface reactions between organic acids and compounds with a variety of functional groups exuded by microbes at the solid-liquid interface, is an integral part of determining the kinetics of microbe-induced dissolution of a given mineral, but mechanisms are still poorly understood [38].

Bibliography

[1] A. Lüttge and P. G. Conrad, "Direct observation of microbial inhibition of calcite dissolution," *Applied and Environmental Microbiology*, vol. 70, no. 3, pp. 1627–1632, 2004.

[2] H. J. Busscher and A. H. Weerkamp, "Specific and non-specific interactions in bacterial adhesion to solid substrata," *FEMS Microbiology Letters*, vol. 46, no. 2, pp. 165–173, 1987.

[3] S. K. Lower, C. J. Tadanier, and M. F. Hochella, "Measuring interfacial and adhesion forces between bacteria and mineral surfaces with biological force microscopy," *Geochimica et Cosmochimica Acta*, vol. 64, no. 18, pp. 3133–3139, 2000.

[4] S. K. Lower, J. Hochella, Michael F., and T. J. Beveridge, "Bacterial recognition of mineral surfaces: Nanoscale interactions between Shewanella and alpha -FeOOH," *Science*, vol. 292, no. 5520, pp. 1360–1363, 2001.

[5] S. K. Lower, "Directed natural forces of affinity between a bacterium and mineral," *Am J Sci*, vol. 305, no. 6-8, pp. 752–765, 2005.

[6] N. Ohmura, K. Kitamura, and H. Saiki, "Selective adhesion of Thiobacillus

ferrooxidans to pyrite," *Appl. Environ. Microbiol.*, vol. 59, no. 12, pp. 4044–4050, 1993.

[7] N. Ohmura, K. Tsugita, J. I. Koizumi, and H. Saika, "Sulfur-binding protein of flagella of Thiobacillus ferrooxidans," *J. Bacteriol.*, vol. 178, no. 19, pp. 5776–5780, 1996.

[8] R. Arredondo, A. Garcia, and C. A. Jerez, "Partial removal of lipopolysaccharide from Thiobacillus ferrooxidans affects its adhesion to solids," *Appl. Environ. Microbiol.*, vol. 60, no. 8, pp. 2846–2851, 1994.

[9] A. Lüttge, "Etch pit coalescence, surface area, and overall mineral dissolution rates," *American Mineralogist*, vol. 90, no. 11-12, pp. 1776–1783, 2005.

[10] L. Hall-Stoodley, J. W. Costerton, and P. Stoodley, "Bacterial biofilms: from the natural environment to infectious diseases," *Nat Rev Micro*, vol. 2, no. 2, pp. 95–108, 2004.

[11] M. C. M. van Loosdrecht, W. Norde, and A. J. B. Zehnder, "Physical chemical description of bacterial adhesion," *J Biomater Appl*, vol. 5, no. 2, pp. 91–106, 1990.

[12] T. R. Neu and K. C. Marshall, "Bacterial polymers: Physicochemical aspects of their interactions at interfaces," *J Biomater Appl*, vol. 5, no. 2, pp. 107–133, 1990.

[13] S. A. Welch and P. Vandevivere, "Effect of microbial and other naturally occurring polymers on mineral dissolution," *Geomicrobiology Journal*, vol. 12, no. 4, pp. 227 – 238, 1994.

[14] P. Devasia, K. A. Natarajan, D. N. Sathyanarayana, and G. R. Rao, "Surface chemistry of Thiobacillus ferrooxidans relevant to adhesion on mineral surfaces," *Appl. Environ. Microbiol.*, vol. 59, no. 12, pp. 4051–4055, 1993.

[15] J. Olsson, P.-O. Glantz, and B. Krasse, "Surface potential and adherence of oral streptococci to solid surfaces," *European Journal of Oral Sciences*, vol. 84, no. 4, pp. 240–242, 1976.

[16] D. C. Savage and M. Fletcher, eds., *Bacterial Adhesion: Mechanisms and Physiological Significance*. New york: Plenum Press, 1985.

[17] M. C. M. van Loosdrecht, J. Lyklema, W. Norde, and A. J. B. Zehnder, "Bacterial adhesion: A physicochemical approach," *Microbial Ecology*, vol. 17, pp. 1–15, 1989.

[18] K. Hori and S. Matsumoto, "Bacterial adhesion: From mechanism to control," *Biochemical Engineering Journal*, vol. 48, pp. 424 – 434, 2010.

[19] J. W. Costerton, G. Cook, M. Shirtliff, P. Stoodley, and M. Pasmore, "Biofilms, biomaterials and device-related infections," in *Biomaterials In Science: An Introduction to Materials in Medicine* (B. D. Ratner, A. S. Hoffman, F. J. Schoen, and J. E. Lemons, eds.), London: Elsevier, 2004.

[20] D. De Beer and P. Stoodley, "Microbial biofilms," in *The Prokaryotes*, New York: Springer, 2006.

[21] W. W. Barker, S. A. Welch, and J. F. Banfield, "Biogeochemical weathering of silicate minerals," in *Geomirobiology: Interactions Between Microbes and Minerals; Reviews in Mineralogy* (J. F. Banfield and K. H. Nealson, eds.), vol. 35, pp. 391–428, Washington D.C.: The Mineralogical Society of America, 1997.

[22] L. J. Liermann, B. E. Kalinowski, S. L. Brantley, and J. G. Ferry, "Role of bacterial siderophores in dissolution of hornblende," *Geochimica et Cosmochimica Acta*, vol. 64, no. 4, pp. 587–602, 2000.

[23] R. M. Donlan, "Biofilms: Microbial life on surfaces," *Emerging Infectious Diseases*, vol. 8, no. 9, pp. 881–890, 2002.

[24] W. W. Barker, S. A. Welch, S. Chu, and J. F. Banfield, "Experimental observations of the effects of bacteria on aluminosilicate weathering," *American Mineralogist*, vol. 83, pp. 1551–1563, 1998.

[25] H. L. Buss, A. Lüttge, and S. L. Brantley, "Etch pit formation on iron silicate surfaces during siderophore-promoted dissolution," *Chemical Geology*, vol. 240, no. 3-4, pp. 326–342, 2007.

[26] L. J. Liermann, A. S. Barnes, B. E. Kalinowski, X. Zhou, and S. L. Brantley, "Microenvironments of pH in biofilms grown on dissolving silicate surfaces," *Chemical Geology*, vol. 171, no. 1-2, pp. 1–16, 2000.

[27] P. Vandevivere, S. A. Welch, W. J. Ullman, and D. L. Kirchman, "Enhanced dissolution of silicate minerals by bacteria at near-neutral ph," *Microbial Ecology*, vol. 27, pp. 241–251, 1994.

[28] D. Jacobson, Andrew and L. Wu, "Microbial dissolution of calcite at T = 28 °C and ambient pCO_2," *Geochimica et Cosmochimica Acta*, vol. 73, pp. 2314–2331, 2009.

[29] H. L. Ehrlich, "Geomicrobiology: its significance for geology," *Earth-Science Reviews*, vol. 45, no. 1-2, pp. 45–60, 1998.

[30] W. W. Barker and J. F. Banfield, "Zones of chemical and physical interaction at interfaces between microbial communities and minerals: A model," *Geomicrobiology Journal*, vol. 15, no. 3, pp. 223 – 244, 1998.

[31] H. L. Ehrlich, "How microbes influence mineral growth and dissolution," *Chemical Geology*, vol. 132, no. 1-4, pp. 5–9, 1996.

[32] W. J. Ullman, D. L. Kirchman, S. A. Welch, and P. Vandevivere, "Laboratory evidence for microbially mediated silicate mineral dissolution in nature," *Chemical Geology*, vol. 132, no. 1-4, pp. 11–17, 1996.

[33] C. Amrhein and D. L. Suarez, "The use of a surface complexation model to describe the kinetics of ligand-promoted dissolution of anorthite," *Geochimica et Cosmochimica Acta*, vol. 52, no. 12, pp. 2785–2793, 1988.

[34] P. C. Bennett, "Quartz dissolution in organic-rich aqueous systems," *Geochimica et Cosmochimica Acta*, vol. 55, no. 7, pp. 1781–1797, 1991.

[35] S. A. Welch, A. E. Taunton, and J. F. Banfield, "Effect of microorganisms and microbial metabolites on apatite dissolution," *Geomicrobiology Journal*, vol. 19, no. 3, pp. 343–367, 2002.

[36] S. A. Welch and W. J. Ullman, "The effect of organic acids on plagioclase dissolution rates and stoichiometry," *Geochimica et Cosmochimica Acta*, vol. 57, no. 12, pp. 2725–2736, 1993.

[37] L. Hersman, T. Lloyd, and G. Sposito, "Siderophore-promoted dissolution of hematite," *Geochimica et Cosmochimica Acta*, vol. 59, no. 16, pp. 3327–3330, 1995.

[38] J. F. Banfield and R. J. Hamers, "Processes at minerals and surfaces with relevance to microorganisms and prebiotic synthesis," *Reviews in Mineralogy and Geochemistry*, vol. 35, no. 1, pp. 81–122, 1997.

[39] B. J. Little, P. A. Wagner, and Z. Lewandowski, "Spatial relationships between bacteria and mineral surfaces," in *Geomicrobiology of Silicate Mineral Weathering, in Geomirobiology: Interactions Between Microbes and Minerals; Reviews in Mineralogy* (J. F. Banfield and K. H. Nealson, eds.), vol. 35, pp. 123–159, Washington D.C.: The Mineralogical Society of America, 1997.

[40] A. de los Ríos, J. Wierzchos, L. G. Sancho, and C. Ascaso, "Acid microenvironments in microbial biofilms of antarctic endolithic microecosystems," *Environmental Microbiology*, vol. 5, no. 4, pp. 231–237, 2003.

[41] M. Kühl and B. B. Jørgensen, "Microsensor measurements of sulfate reduction and sulfide oxidation in compact microbial communities of aerobic biofilms," *Appl. Environ. Microbiol.*, vol. 58, no. 4, pp. 1164–1174, 1992.

[42] C. M. Santegoeds, T. G. Ferdelman, G. Muyzer, and D. de Beer, "Structural and functional dynamics of sulfate-reducing populations in bacterial biofilms," *Appl. Environ. Microbiol.*, vol. 64, no. 10, pp. 3731–3739, 1998.

[43] N. B. Ramsing, M. Kühl, and B. B. Jørgensen, "Distribution of sulfate-reducing bacteria, o2, and h2s in photosynthetic biofilms determined by oligonucleotide probes and microelectrodes.," *Appl. Environ. Microbiol.*, vol. 59, no. 11, pp. 3840–3849, 1993.

[44] C. M. Santelli, S. A. Welch, H. R. Westrich, and J. F. Banfield, "The effect of fe-oxidizing bacteria on fe-silicate mineral dissolution," *Chemical Geology*, vol. 180, no. 1-4, pp. 99–115, 2001.

[45] R. G. Arnold, T. J. DiChristina, and M. R. Hoffmann, "Reductive dissolution of Fe(iii) oxides by Pseudomonas sp. 200," *Biotechnology and Bioengineering*, vol. 32, no. 9, pp. 1081–1096, 1988.

[46] C. O. Obuekwe, D. W. S. Westlake, and F. D. Cook, "Effect of nitrate on reduction of ferric iron by a bacterium isolated from crude oil," *Canadian Journal of Microbiology*, vol. 27, no. 7, pp. 692–697, 1981.

[47] C. O. Obuekwe, D. W. S. Westlake, and J. A. Plambeck, "Evidence that available energy is a limiting factor in the bacterial corrosion of mild steel by a Pseudomonas sp," *Canadian Journal of Microbiology*, vol. 33, no. 3, pp. 272–275, 1987.

[48] M. C. Grantham, P. M. Dove, and T. J. Dichristina, "Microbially catalyzed dissolution of iron and aluminum oxyhydroxide mineral surface coatings," *Geochimica et Cosmochimica Acta*, vol. 61, no. 21, pp. 4467–4477, 1997.

[49] K. J. Edwards, B. M. Goebel, T. M. Rodgers, M. O. Schrenk, T. M. Gihring, M. M. Cardona, M. M. McGuire, R. J. Hamers, N. R. Pace, and J. F. Banfield, "Geomicrobiology of pyrite (FeS_2) dissolution: Case study at iron mountain, california," *Geomicrobiology Journal*, vol. 16, no. 2, pp. 155–179, 1999.

[50] C.-y. Jia, D.-z. Wei, W.-g. Liu, C. Han, S.-l. Gao, and Y.-j. Wang, "Selective adsorption of bacteria on sulfide minerals surface," *Transactions of Nonferrous Metals Society of China*, vol. 18, no. 5, pp. 1247–1252, 2008.

[51] A. K. Friis, T. A. Davis, M. M. Figueira, J. Paquette, and A. Mucci, "Influence of bacillus subtilis cell walls and EDTA on calcite dissolution rates and crystal surface features," *Environmental Science and Technology*, vol. 37, no. 11, pp. 2376– 2382, 2003.

[52] L. Wu, A. D. Jacobson, and M. Hausner, "Characterization of elemental release during microbe-granite interactions at T=28 °C," *Geochimica et Cosmochimica Acta*, vol. 72, no. 4, pp. 1076–1095, 2008.

[53] L. Wu, A. D. Jacobson, H.-C. Chen, and M. Hausner, "Characterization of elemental release during microbe-basalt interactions at T= 28 °C," *Geochimica et Cosmochimica Acta*, vol. 71, no. 9, pp. 2224–2239, 2007.

Chapter 3

Influence of Microbes on Limestone Weathering

Sulu-Gambari, Fatimah[i*] and **Mucci,** Alfonso[i] and **Frigon,** Dominic[ii]

3.1 Abstract

The dissolution kinetics of Iceland Spar calcite rhombobedra was investigated in low-ionic strength (10^{-2} M) NaCl solutions at ambient pCO_2 and 25 °C, following inoculation with a natural bacterial consortium. The effect of solution chemistry (e.g. the growth media and presence of phosphate) was also investigated. Total calcium concentration, alkalinity and pH were monitored during the dissolution process and fit to an empirical rate law. Dissolution rates in biotic reactors were not seen to increase relative to abiotic phosphate-free or phosphate-containing reactors. Calcium release rates were lower in phosphate-containing reactors than in phosphate-free reactors. Bacterial attachment to crystal surfaces, as observed by fluorescence microscopy, increased in the

[i]Earth and Planetary Sciences, McGill University, Montréal
[*]Corresponding author: ✉ fatimah.sulu-gambari@mail.mcgill.ca
[ii]Civil Engineering, McGill University, Montréal

presence of freely-available phosphate relative to reactors in which the phosphate had been pre-adsorbed to calcite rhombs.

Keywords calcite, *Actinobacteria*, dissolution kinetics, alkalinity, phosphate, saturation state

3.2 Introduction

Geochemical, fossil and genetic data highlight the importance of microbe-mineral interactions in early earth history, particularly with respect to cycling and distribution of life-supporting nutrients and major lithogenic elements [1]. Microorganisms are ubiquitous in natural aquatic environments and often colonise mineral surfaces in the form of biofilms [2]. Hence, bacteria can influence the rates of rock weathering by modifying the chemistry of the solution at mineral interfaces by secreting metabolites or specific ligands that increase the mobility of mineral constituents [3–5].

Calcite ($CaCO_3$) is the most stable calcium carbonate polymorph under earth surface conditions and it is a ubiquitous and highly reactive sedimentary mineral [6]. Several reports of bacterially-mediated precipitation of calcite have been published to date (e.g. [7–10]) but there is a very limited amount of literature on their influence on calcite dissolution rates [11] and those reports are contradictory (e.g. [12–16]). Moreover, model organisms (e.g. [17–22]) or inactive cells (e.g. [14]) were used in these studies and thus, results may not be proper analogues of natural processes. In this study, weathering conditions were simulated by inoculating solutions containing calcite cleavage rhombohedra with a natural consortium of bacteria and dissolution rates were measured in the presence and absence of bacteria in pure water, phosphate-free and phosphate growth media.

3.3 Materials and Methods

3.3.1 Characterisation and Preparation of Weathered Samples

Weathered rock samples were collected from thermally-altered Trenton Carbonates on Mt. Royal in Montréal. Damp, organic-rich sediments were collected along the Ormsted Trail, as indicated on Figure 3.1. Samples were scraped from rock wedges where limestone outcropped. Chemical analysis of the sample material included X-Ray diffraction spectrometry (XRD), X-ray fluorescence spectrometry (XRF), organic carbon and total carbon. XRD analyses were carried out on a Rigaku D/MAX 2400 12kW rotating anode diffractometer at L'Université du Québec à Montréal (UQAM), Canada (Cu-Kα radiation, 0.00828 ° step-size, counting time of 2 seconds per step). Major element analyses were performed using XRF. X-ray fluorescence of whole rock powders was carried out with a Philips PW2440 4kW automated XRF spectrometer system at the Trace Element Analysis Laboratories, McGill University, Canada. Major elements (SiO_2, TiO_2, $Al_2 2O_3$, Fe_2O_3, MnO, MgO, CaO, Na_2O, K_2O, P_2O_5) and trace elements (Ba, Ce, Co, Cr, Cu, Ni, Sc, V, Zn) were analysed in 32-mm diameter fused beads. Loss-on-ignition (LOI) was measured on a portion of the powder before lithium borate fusion. XRD and XRF analyses were conducted with detection limits of 5%. Weathered samples were freeze-dried and homogenised (by grinding in an agate mortar). Total carbon and nitrogen content of the sediments were determined using a Carlo-Erba NC 2500 elemental analyser. The absolute instrumental reproducibility of these analyses was estimated at 0.1% for C_{TOT} and 0.3% for N_{TOT} with a reproducibility of 5%. The total inorganic carbon (C_{INORG}) content was analysed on distinct aliquots of the freeze-dried samples using a UIC Coulometrics coulometer, following acidification of the samples and CO_2 extraction. The analytical reproducibility was better than 5%. The total organic carbon (C_{ORG}) content was obtained by subtracting the C_{INORG} from C_{TOT}.

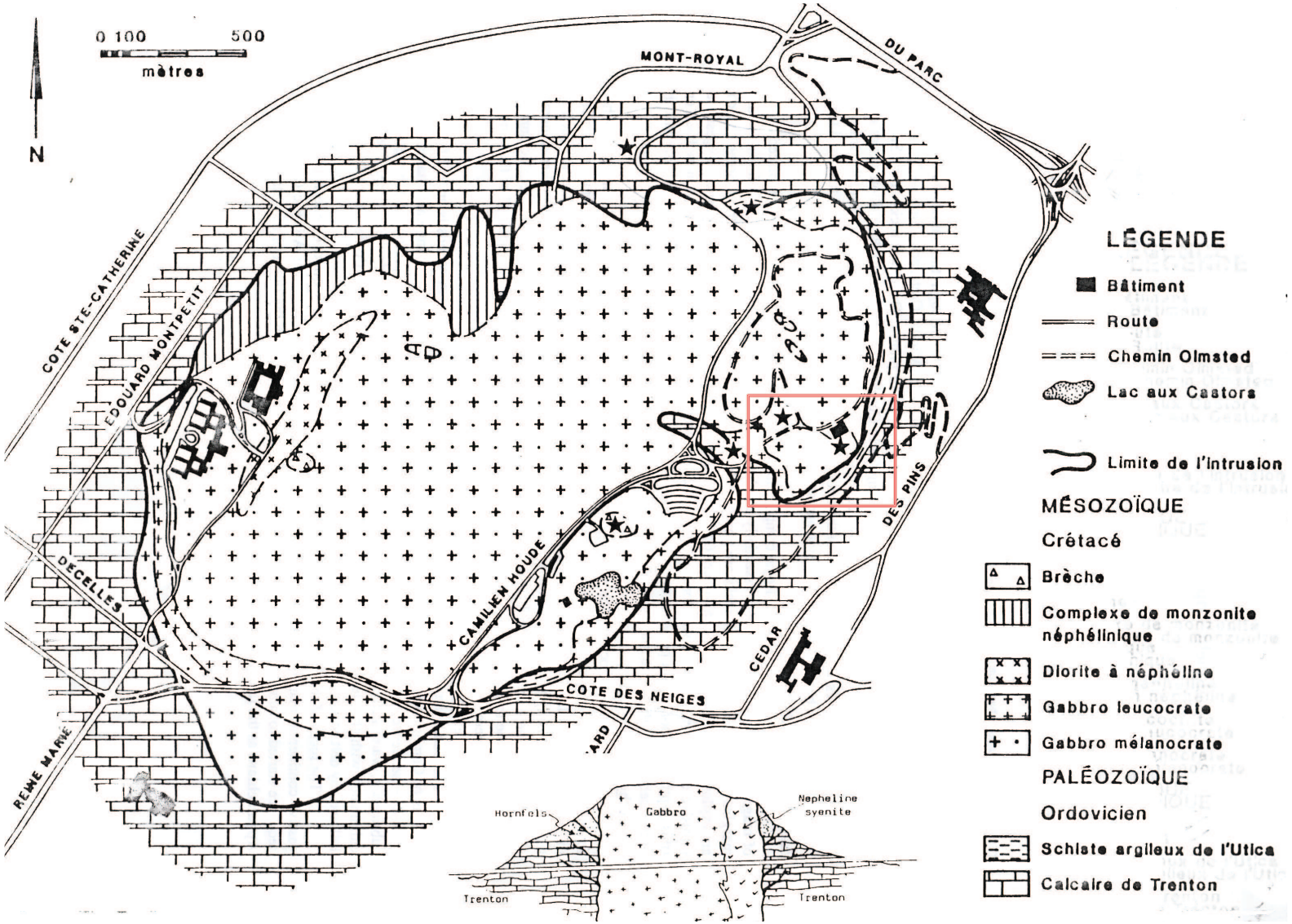

Figure 3.1: Samples were collected along the Ormsted Trail at the intersection of Des Pins and Peel Streets in Montréal.

3.3.2 Microbe Characterisation

Preliminary tests using molecular techniques were used to check for viability and to identify bacterial strains in the samples. This enabled identification of bacteria that thrive in freshwater carbonate systems and allowed the identification of required nutrients for preparation of a suitable growth medium for batch experiments. Applied techniques included diversity fingerprinting techniques such as Polymerase Chain Reaction (PCR)[iii] (see Table 1 for PCR programme) as well as Terminal Restriction Fragment Length Polymorphism (T-RFLP) analysis of the population of interest. Both techniques make use of the 16s rRNA, a conserved Ribosomal RNA sequence common to all prokaryotes [23]. A brief description of each process is provided in Appendix A, including the advantages and limitations of each one.

3.3.3 Characterisation and Preparation of Calcite Rhombs

Ward's® Scientific (non-optical grade) Iceland Spar calcite crystals from Chihuahua, Mexico, were cleaved, using a clamp and razor blade, into smaller rhombohedra of similar sizes to provide templates of a determined surface area[iv] of about 0.5 cm^2/g. They were approximately 5mm in length, 4mm in width and 3mm thick. Crystals were cleaved parallel to natural cleavage planes to expose the $\{10\bar{1}4\}$ face, which is a charge-neutral surface [11]. The rhombs were cleaned in dilute HCl (2%) for 2-3 seconds to remove fine particles, rinsed with acetone[v] to remove dust and debris and quickly rinsed with Milli-Q® water before being dried at 50-70 °C overnight to enable sterilisation. They were subsequently transferred to a dessicator until use.

[iii] Forward primer: 5′ ACT CCT ACG GGA GGC AGC 3′, reverse primer: 5′ GAC GGG CGG TGT GTA CAA 3′.

[iv] Specific surface area calculated from the geometric dimensions of the crystals.

[v] Acetone does not significantly dissolve the calcite crystal surface and can be used as a cleaning agent [24]

3.3.4 Media Preparation

The recipe for W medium was chosen because it is a minimal medium for culturing bacteria, providing only the essential nutrients in limited quantities, thus minimising the inhibitory effect of phosphate and other solutes. It was modified from the recipe given by Atlas (2005) in the Handbook of Media [25] and the trace metal recipe was taken from the mineral salts medium recipe given by Kimbara *et al.* (1989) [26]. Stock solutions of the major media constituents (see Table 3.1) and a separate solution of trace metals (see Table 3.2) were prepared gravimetrically. Stock solutions were 10 times more concentrated than the final experimental/working solutions for W media. Sodium acetate was used as the energy source, as sodium is relatively inert. Solutions were stored in plastic vessels, with the exception of phosphate stock solutions which were stored in glass bottles (solutions were only sterilised immediately prior to use)[vi].

Table 3.1: Modified W-Medium recipe (I = 1.08 $\times 10^{-1}$M (given by PHREEQC using wateq4f.dat)) or (I = 1.6 $\times 10^{-1}$M (given by PHREEQC using llnl.dat))

Constituent	**Working Solution Mass (per L)**	**Concentration**	**Stock Solution Mass (per L)**
$NaCH_3COOH$	10g	0.12M	100g
KH_2PO_4	3g	0.022M	30g
$MgSO_4.7H_2O$	0.5g	2.03 $\times 10^{-3}$M	5g
$CaCl_2.2H_2O$	0.25g	1.7 $\times 10^{-3}$M	2.5g
$(NH_4)_2SO_4$	0.2g	1.5 $\times 10^{-3}$M	2g
$FeSO_4.7H_2O$	10mg (0.01g)	3.6 $\times 10^{-5}$M	100mg

3.3.5 Dissolution Kinetics

Prior to the experiments, glassware was sterilised in an oven at 180 °C for 2 hours. Calcite rhombohedra were mounted at the bottom of 1L beakers and immersed in 500mL of the experimental media solutions. The crystals were fixed using an inert and waterproof silicone sealant, Permatex®, which did not react with the solution constituents or the calcite, hence has no effect on the dissolution rates and solution chemistry [21]. The volume of solution allowed for multiple samplings as the dissolution

[vi]To minimise the adsorption of phosphate on the surface of the vessel.

Table 3.2: Trace Metal Solution recipe (I = 1.8 $\times 10^{-5}$M (given by PHREEQC using llnl.dat, as wateq4f.dat does not contain cobalt or boron))

Constituent	**Working Solution Mass/Volume (per L)**	**Concentration**	**Stock Solution Mass (per L)**
$MgSO_4.7H_2O$	0.01g	4 $\times 10^{-5}$M	0.01g
$FeSO_4.7H_2O$	0.095mg (0.000095g)	3.4 $\times 10^{-7}$M	0.95mg
$CaCO_3$	0.2mg (0.0002g)	2 $\times 10^{-6}$M	2mg
$ZnSO_4.7H_2O$	0.144mg (0.000144g)	5.01 $\times 10^{-7}$M	1.44mg
$CuSO_4.5H_2O$	0.025mg (0.000025g)	1.0 $\times 10^{-7}$M	0.25mg
$CoSO_4.7H_2O$	0.028mg (0.000025g)	10 $\times 10^{-8}$M	0.28mg
H_3BO_3	0.006mg (0.000006g)	10 $\times 10^{-8}$M	0.06mg
Conc acid (H_2SO_4)	51.3μL		

experiment proceeded: approximately 30mL for alkalinity and 10mL for calcium analyses. The alkalinity aliquots were also used for pH measurements. Between 10 and 16 measurements were taken per run. For all experiments, a fluid:mineral mass ratio of 100 (500mL:5g) was adopted (or $\approx$ 200mL/cm^2). This makes variations in calcium concentration easily detectable, and enables precise determination of the dissolution rate. Solutions were allowed to equilibrate with the atmosphere at ambient room temperature (25 °C $\pm$ 2), pressure (1 atm) on a rotary shaker at approximately 120-150 rpm.

3.3.5.1 Abiotic Control Experiments

Rhombohedra were immersed in 10^{-2}M NaCl solutions prepared from the salt and Milli-Q® water. The solutions were autoclaved at 121 °C for 20 minutes prior to the experiments. The beakers were placed on a rotary shaker; otherwise a suspended stir bar was inserted at the bottom of the beaker along with the Iceland Spar calcite crystals and allowed to stand on a magnetic stirrer for the duration of the experiment[vii]. Samples were collected from each beaker with syringes at intervals ranging from a few seconds to a few hours on a five- to seven-day continuum. Aliquots were collected for calcium concentration and alkalinity measurements. Samples for calcium measurements were acidified with (v/v) 1% trace metal grade concentrated HCl to keep the calcium in

[vii]This was used in fewer runs as heat generated by magnetic stirrers caused slight evaporation of the solutions.

solution until analysis.

Control Experiments in Growth Media The first set of control experiments investigated calcite dissolution kinetics in an abiogenic calcite-water-electrolyte system at constant ionic strength (I) and temperature. This was followed by a second set of experiments to monitor calcite dissolution kinetics in the presence of the growth medium. Replicate experiments were conducted in growth media in the presence and absence of phosphate.

3.3.5.2 Bacterial Dissolution Experiments (Nutrient-Limited Metabolism)

A set of calcite dissolution experiments was carried out in phosphate-free and phosphate-limited growth media, in the presence of viable bacteria. This set of experiments investigated the kinetics of biotic dissolution without progressive bacterial growth cycles (i.e. endogenous metabolism). Two different protocols were used. Pristine calcite rhombs were either immersed directly in the growth medium or were pre-treated with a phosphate (NaH_2PO_4) solution to draw the bacteria to their surface[viii]. Phosphate adsorbs strongly to the calcite surface [27, 28]. The phosphate pre-treatment ensured that the survival of the bacteria was limited only by their ability to attach to the crystal surface and did not allow bacteria to solely thrive on the phosphate present in the medium. The inoculums (5g of weathered sample) were then introduced to the system and the bacteria were allowed to colonise the crystal surfaces. Crystals were extracted from solution after 48 hours to determine the bacterial cell-density at their surface. These were stained with DAPI (4',6-diamidino-2-phenylindole), a stain that binds to DNA, and visualised by fluorescence microscopy. Kinetic experiments were conducted with colonised crystals in 10^{-2}M NaCl solutions. The experimental design is shown in Figure 3.2.

[viii] Phosphate is an essential nutrient and bacteria are expected to be drawn to the surface to acquire the adsorbed phosphate.

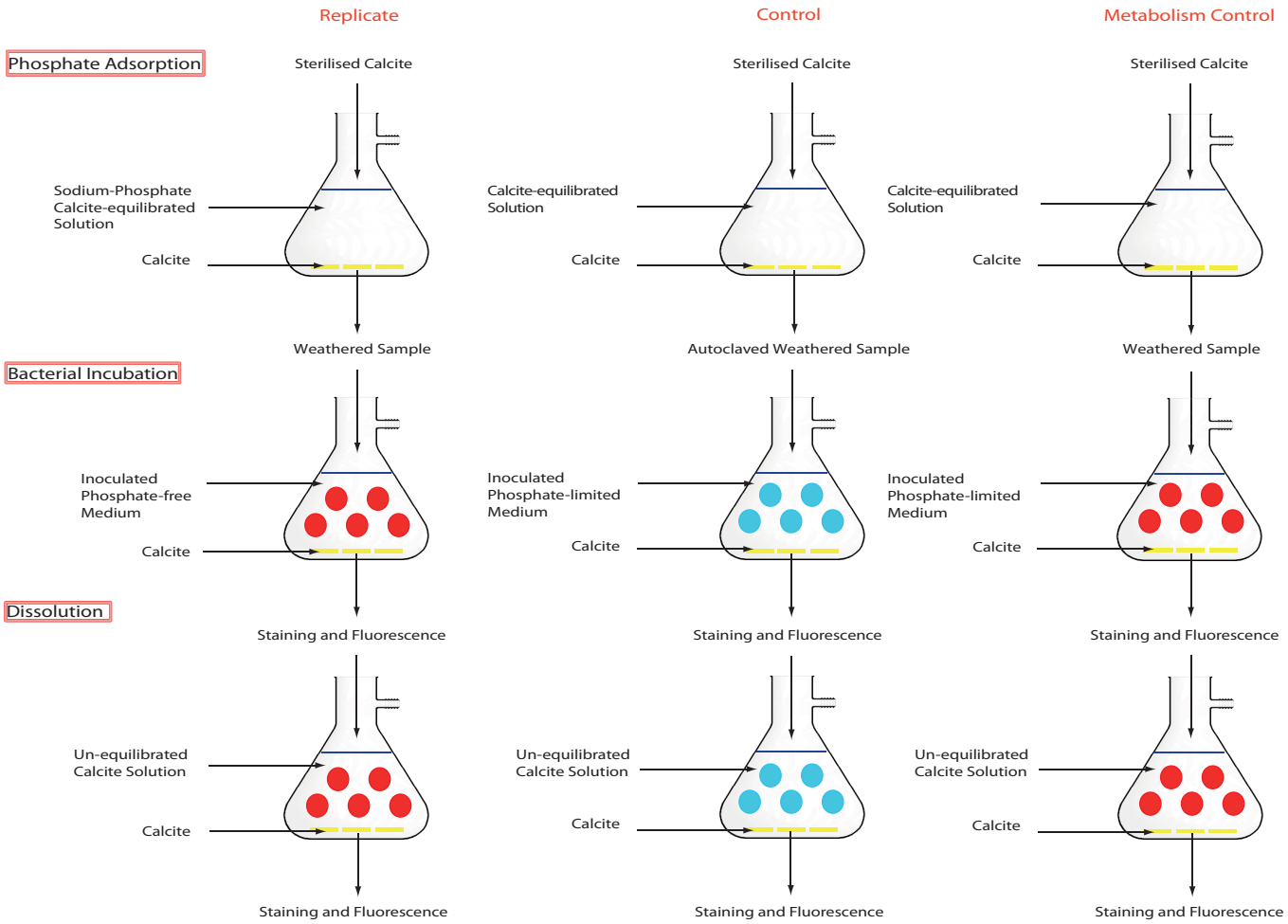

Figure 3.2: Inoculation of medium and dissolution kinetics of calcite crystals. In preliminary experiments, calcite crystals were either pre-treated with a phosphate solution (1mM) before introduction to a phosphate-free medium, or introduced directly into a phosphate-limited medium. Live or autoclaved bacteria were introduced into reactors for a 48-hour incubation period. Following colonisation, the crystals were introduced into 10^{-2}M NaCl solutions for dissolution kinetics measurements.

3.3.5.3 Surface Colonisation Experiments (Growth Metabolism)

An additional set of calcite dissolution experiments was carried out in phosphate-free and phosphate-limited growth media, in the presence of viable bacteria. This second set, unlike the first (Figure 3.2) during which the calcite dissolution kinetics was monitored, was carried out to observe the effect of the bacterial growth metabolism, and thus, fewer data points were collected. Again, two different protocols were used. Smaller reactors were used with a smaller volume of solution and crystals; 1g of crystal rhombs were immersed in 100mL solutions, to which 1g of weathered sample was eventually added. Media was replaced in each reactor for four cycles or runs (R1-R4) at 48-72-hour intervals, allowing the bacteria to grow through each cycle. Finally on the fifth cycle (R5), media were replaced by a 0.01M NaCl solution. Crystals were extracted from the media following R4 and R5 for staining and microscopy. The experimental design is shown in Figure 3.3.

3.3.6 Analytical Methods

3.3.6.1 Calcium Analyses

Calcium concentrations in solution were measured using atomic absorption spectrometry (AAS). A Perkin Elmer AA-100 Atomic Absorption Flame Emission Spectrometer was used in conjunction with a calcium cathode lamp and an air-acetylene flame. The instrumental detection limit is 0.092ppm (2.29×10^{-6}M) with a reproducibility better than 5%. Standards were prepared from dilution of a 1000ppm Plasmacal® inductively coupled plasma (ICP) calcium standard in 0.01 M NaCl (Table 3.3). The range of standards prepared for AAS analysis was dependent on the anticipated concentration of calcium in samples[ix] (i.e. 0.1-40ppm). It should be noted that matrix effects on the AAS signal do not generally occur when samples contain organic compounds, although high phosphate concentrations can cause interference, as it may complex with the ion of interest, forming precipitates. The total calcium concentrations of the experimental solutions were used to calculate the rate of dissolution, as discussed in section 3.3.5.

[ix] and should cover the linear response range of the instrument

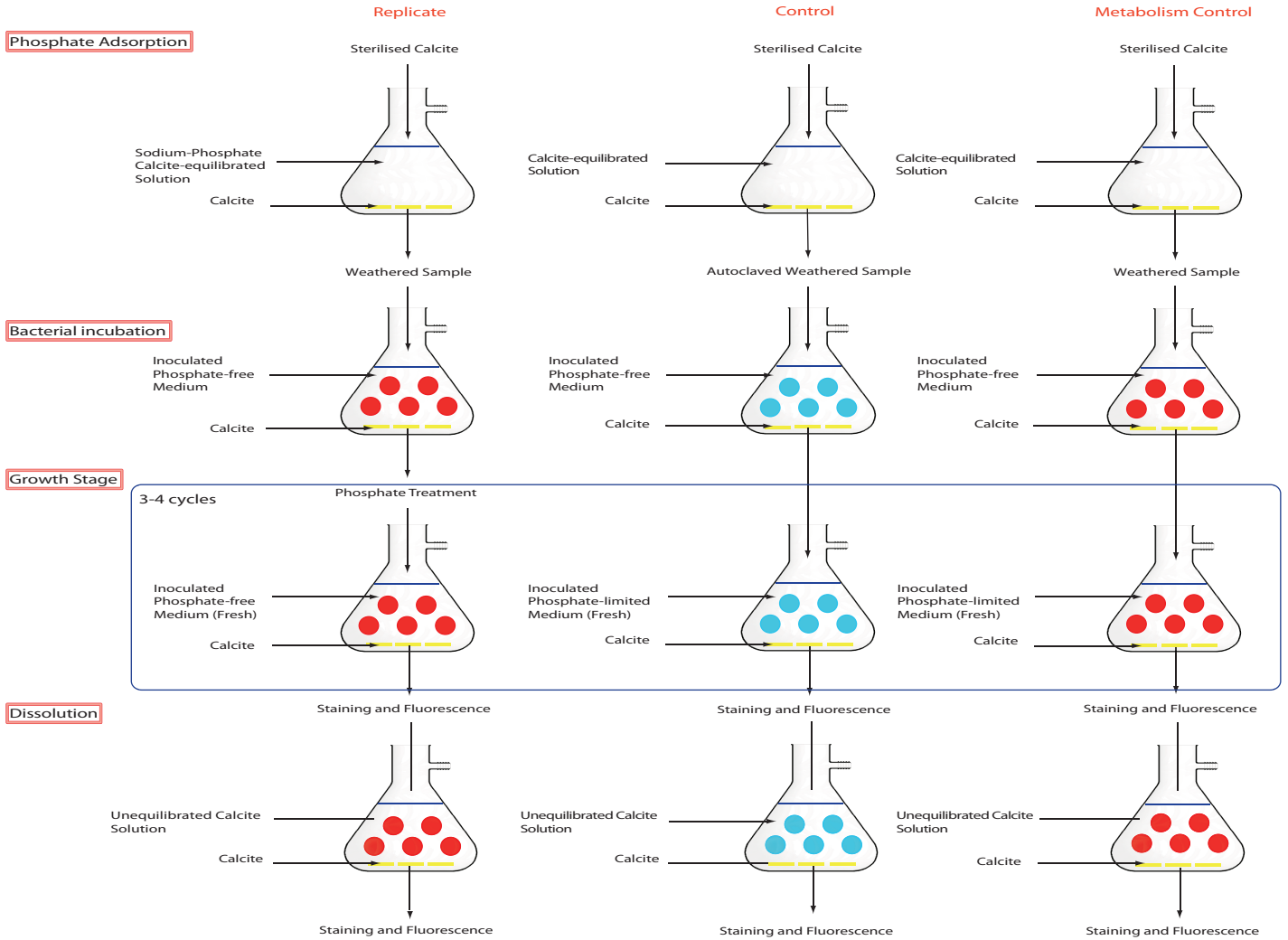

Figure 3.3: Inoculation of medium and dissolution kinetics of calcite crystals. In preliminary experiments, calcite crystals were either pre-treated with a phosphate solution (1mM) before introduction to a phosphate-free medium, or introduced directly into a phosphate-limited medium. Live or autoclaved bacteria were introduced into reactors for a 48-72-hour incubation period. The solutions were sampled during the incubation. Growth media were replaced 4 times. After the fourth cycle, the crystals were introduced into 10^{-2}M NaCl solutions for dissolution kinetics measurements.

Table 3.3: Table of AAS Standards (0.10ppm, 0.25ppm and 0.50ppm solutions made using prepared 10ppm standard)

Standard	**End Volume Standard**	**Concentration Stock Solution**	**Volume Stock Solution Added (per L)**
Blank	100mL		
0.10ppm	50mL	10ppm	0.5mL
0.25ppm	50mL	10ppm	1.25mL
0.50ppm	50mL	10ppm	2.50mL
1.00ppm	50mL	1000ppm	0.05mL
2.50ppm	50mL	1000ppm	0.125mL
5.00ppm	100mL	1000ppm	0.5mL
10.0ppm	50mL	1000ppm	0.5mL

3.3.6.2 Alkalinity Titrations

Total alkalinity titrations were carried out using a Radiometer Titralab 865 automated potentiometric titrator and a combination glass electrode (GK2401C) with a dilute HCl solution (0.003N). The reproducibility of measurements was better than 0.5%. Alkalinity of the solutions was monitored as a check of the stoichiometry and/or kinetics of the dissolution process, but also to calculate the saturation state of the solution at every sampling interval. Measured alkalinity was compared to the theoretical values returned by PHREEQC using measured calcium concentrations and pH as input parameters. These values were comparable to within 100μM. Alkalinity standards were prepared gravimetrically with a dried Na_2CO_3 standard salt to concentrations close to the samples.

3.3.6.3 pH Measurements

pH measurements were carried out using a Radiometer® Analytical combination glass electrode (GK2401C) in conjunction with a Radiometer® M84 pH/millivolt-meter, or a TitraLab® TIM 865 Titration system. For both apparatus, glass pH combination electrodes were calibrated using three NIST-traceable buffer solutions of pHs 4.00, 7.00 and 10.00 at 25 °C. The potentials returned from the three buffers were plotted as a

function of the assigned pH and the relationship fit to a linear equation of the form:

$$y = mx + c \tag{3.1}$$

where m, the slope of the fit, is the Nernstian response of the electrode and c is the intercept (E∘'). The pH of a solution, y, was calculated from the fit and its potential returned by the pH-metre and x could be calculated as the pH of said solution. Calibrations were carried out before and after measurements and until the potential (EP) readings were reproducible to ±0.2mV for each buffer. The sample pH measurements were reproducible to ±0.005.

3.3.6.4 Phosphate Measurements

The soluble reactive phosphate (SRP) concentration in solution was measured using a HP model 8453A diode-array UV-visible spectrophotometer, with an instrumental detection limit of 0.5μg-P/L, according to the protocol described by Koroleff (1976), adapted from the method of Murphy and Riley (1962), with a reproducibility better than 5%.

3.3.6.5 Microscopy

Rhombs salvaged from bacterial attachment experiments were stained using DAPI. The stain was prepared in a 0.85% saline solution to prevent the bacteria from experiencing an ionic shock. Stained rhombs were examined by fluorescence microscopy, using an Olympus® BX51 system microscope in conjunction with an X-Cite® 120PQ fluorescence Illumination system.

3.3.7 Modelling of Speciation and Dissolution

The saturation state of the experimental solution prior to and during the dissolution experiments were estimated using PHREEQC with the WATEQ4F.dat (for saline solutions) and LLNL.dat (for media) thermodynamic databases. Calcium, pH and alkalinity, as well as constituents of the growth media (when appropriate) were used as input parameters to the model. PHREEQC is a collective name for different versions of

a speciation algorithm developed by Parkhurst and Appelo [29] that allows for the modelling of basic freshwater systems. Equilibration and dissolution kinetics were modelled with PHREEQCI version 2 without the effect of stirring. Hence, the modelling of kinetics here simulates weathering rather than induced dissolution.

3.4 Results and Discussion

3.4.1 Characterisation of the Inoculum Sample

According to the XRD analysis, the collected weathered samples were composed mainly of quartz and calcite. Samples also contained plagioclase (anorthosite and albite) and some orthoclase feldspar (Figures 3 and 4). The total carbon content was low, between 0.5 and 12% of which 0.45% was organic. Bulk sample XRF analyses, like the XRD results, indicated that samples were silica (≈51wt% SiO_2) and calcium (≈12-16wt%) rich. Samples contained significant amounts of Fe (2.5-5wt% Fe_2O_3) and traces of phosphate (0.15-1.2wt% P_2O_5), nickel (21ppm) and cobalt (12ppm). Results of the total carbon and XRF analyses are reported in Appendix B (Figure 2 (A) and (B), respectively).

Organisms in samples were compared to known 16s rRNA sequences in public databases[x]. Identified microbes belonged to the phylum *Actinobacteria*. Other organisms were 'unclassified'. *Actinobacteria* are gram-positive, soil-dwelling microorganisms, with a high guanine-cytosine (GC) content (>55 mol%). They are widely distributed in aquatic and terrestrial ecosystems, are divided into 39 families and 130 genera [30] and play important roles in organic matter decomposition and humus formation. A phylogenetic tree was also constructed, using cloning libraries, which depicted that within this class, the sequences are further classified into four genera of *Actinobacteria* namely *Actinomycetaceae*, *Propionibacteriaceae*, *Glycomycetaceae* and *Nocardiaceae*. See phylogenetic tree in Appendix C.

[x] A list of databases can be found at `http://www.ncbi.nlm.nih.gov/guide/all/#databases`

3.4.2 Calcite Dissolution Kinetics

3.4.2.1 Calite Dissolution Rate

The calcite dissolution rate was calculated as

$$Rate = \frac{\Delta \left[Ca^{2+}\right]}{tA} \tag{3.2}$$

where the rate (mol.m^{-2}.hr^{-1}) is estimated from the change in the calcium concentration ($\Delta\ [Ca^{2+}]$) over two sampling time intervals divided by the lapsed time (t) and normalised to the total surface area of the calcite crystals (A) exposed to the solution [14]. The uncertainty on the rate measurements is estimated at ± 5% based on the cumulative errors of the calcium analyses (± 3%) and crystal size measurements (± 3%) (*ibid*). The rate estimates were not very reproducible but were generally better than 50%. No corrections were made for changes in specific surface resulting from dissolution over the course of the experiments. For comparison, dissolution rates were plotted as a function of the saturation state (Ω) of the experimental solutions and expressed as:

$$Rate = k\,(1 - \Omega)^n \tag{3.3}$$

where Ω is calculated by dividing the ion activity quotient Q by the thermodynamic solubility constant (K^0_{sp}) of calcite, where $K^0_{sp} = 10^{-8.48}$ [31].

3.4.2.2 Elemental Release Rates (Nutrient-Limited Metabolism)

Equilibration and abiotic experiments were compared to simulations in PHREEQC. Values for final solution calcium concentrations, pH and alkalinity in pure water and nutrient media were compared to those of empirical analogues (i.e. solutions of identical composition in equilibrium with calcite) returned by PHREEQC. Tables 3.4 to 3.9 report calcium concentrations, alkalinity, pH and reaction rate data for experiments in water, phosphate-free and phosphate-limited media as well as for batch experiments. The instantaneous calcium release rates in water, media and in the presence of bacteria decreased exponentially with time. Dissolution rates were lower in abiotic phosphate-containing reactors (Table 3.6) than in the abiotic phosphate-free reactors (Table 3.5). A comparison of the dissolution kinetics in abiotic and biotic systems, in the

Table 3.4: Abiotic Calcite Dissolution Kinetics in phosphate-free NaCl solution

Reactor	**Description**	**Time (Hours)**	**Ca^{2+}** (M)	**Alk_{tot}** (μM)	pH	**Inst. Rate** ($mol.m^{-2}.h^{-1}$)	Ω_{ca}	**SRP** (μM)
C	crystals + NaCl + water	0	4.14E-06	n.a	5.59	0	n.a	n.a
		0.008333	3.84E-06	n.a	5.71	n.a	n.a	n.a
		0.016667	2.20E-06	n.a	5.55	n.a	n.a	n.a
		0.033333	2.72E-06	n.a	5.79	8.38E-06	n.a	n.a
		0.083333	5.81E-06	n.a	5.83	1.65E-05	n.a	n.a
		0.166667	1.03E-05	n.a	6.07	1.45E-05	n.a	n.a
		0.5	2.61E-05	n.a	6.54	1.26E-05	n.a	n.a
		1	4.89E-05	n.a	6.89	1.22E-05	n.a	n.a
		3	0.000125	n.a	7.35	1.01E-05	n.a	n.a
		6	0.000228	264.7	7.61	9.12E-06	0.0146	n.a
		12	0.000355	588.4	7.83	5.68E-06	0.084	n.a
		24	0.000504	864.2	7.97	3.29E-06	0.239	n.a
		48	0.000588	464.7	8.05	9.40E-07	0.182	n.a
		72	0.000614	1096	8.13	2.83E-07	0.532	n.a
		96	0.000572	1128	8.10	n.a	0.481	n.a
		120	0.000588	1131	8.11	1.75E-07	0.509	n.a
	PHREEQC		**0.000593**	**1208**	**8.246**		1.00	

Table 3.5: Calcite Dissolution Kinetics in $\frac{1}{10}$ Phosphate-free Media

Reactor	**Description**	**Time (Hours)**	**Ca^{2+}** (M)	**Alk_{tot}** (μM)	pH	**Inst. Rate (mol.m^{-2}.h^{-1})**	**Ω_{ca}**	**SRP** (μM)
D	crystals + NaCl + Phosphate-free Medium	0	4.29E-06	n.a.	6.16	0	n.a.	n.a
		0.008333	4.67E-06	n.a.	6.05	5.25E-05	n.a.	n.a
		0.016667	4.24E-06	n.a.	6.04	n.a	n.a.	n.a
		0.033333	3.27E-06	n.a.	6.06	n.a	n.a.	n.a
		0.083333	5.66E-06	n.a.	6.28	5.60E-05	n.a.	n.a
		0.166667	8.46E-06	n.a.	6.43	3.92E-05	n.a.	n.a
		0.5	3.43E-05	n.a.	7.08	9.06E-05	n.a.	n.a
		1	7.41E-05	85.2	7.58	9.32E-05	0.0014	n.a
		3	0.000213	206.6	7.74	8.11E-05	0.014	n.a
		6	0.000283	505.7	7.89	2.74E-05	0.067	n.a
		12	0.000397	726.9	8.14	2.21E-05	0.23	n.a
		24	0.000518	993.5	8.25	1.18E-05	0.54	n.a
		48	0.000616	1297	8.34	4.78E-06	1.04	n.a
	PHREEQC		**0.000975**	**1079**	**8.183**		1.00	
Reactor	**Description**	**Time (Hours)**	**Ca^{2+}** (M)	**Alk_{tot}** (μM)	pH	**Inst. Rate (mol.m^{-2}.h^{-1})**	**Ω_{ca}**	**SRP** (μM)
F	crystals + NaCl + Phosphate-free Medium	0	2.25E-06	0	6.29	0	n.a	n.a
		0.016667	2.62E-06	0	6.18	2.63E-06	n.a	n.a
		0.083333	6.36E-06	0	6.35	6.57E-06	n.a	n.a
		0.25	1.93E-05	0	6.73	9.05E-06	n.a	n.a
		0.5	3.64E-05	0	7.01	8.02E-06	n.a	n.a
		1	7.00E-05	95.4	7.38	7.86E-06	0.00096	n.a
		6	0.000293	292.6	7.89	5.22E-06	0.04	n.a
		12	0.000454	850.2	7.98	3.13E-06	0.22	n.a
		24	0.000570	1096	8.23	1.13E-06	0.62	n.a
	PHREEQC		**0.000975**	**1079**	**8.183**		1.00	

Table 3.6: Calcite Dissolution Kinetics in $\frac{1}{10}$ Phosphate-limited Media

Reactor	**Description**	**Time (Hours)**	**Ca^{2+}** (M)	**Alk_{tot}** (μM)	pH	**Inst. Rate (mol.m^{-2}.h^{-1})**	**Ω_{ca}**	**SRP** (μM)
E	crystals + NaCl + Phosphate Medium	0	1.87E-06	n.a	6.57	0	n.a	n.a
		0.008333	1.50E-06	n.a	6.55	n.a	n.a	n.a
		0.016667	1.80E-06	n.a	6.41	3.15E-06	n.a	n.a
		0.033333	2.70E-06	n.a	6.49	4.73E-06	n.a	n.a
		0.083333	4.97E-06	n.a	6.56	3.98E-06	n.a	n.a
		0.166667	8.83E-06	n.a	6.67	4.07E-06	n.a	n.a
		0.5	2.79E-05	n.a	7.05	5.02E-06	n.a	n.a
		1	6.08E-05	143.5	7.29	5.77E-06	0.00103	n.a
		3	0.000199	234.8	7.67	6.09E-06	0.013	n.a
		6	0.000240	298.6	7.89	1.17E-06	0.033	n.a
		12	0.000337	456.7	8.02	1.43E-06	0.095	n.a
		24	0.000405	799.3	8.13	4.92E-07	0.26	n.a
		48	0.000514	1013	8.22	3.98E-07	0.52	n.a
	PHREEQC		**0.000832**	**5455**	**8.155**		1.00	
Reactor	**Description**	**Time (Hours)**	**Ca^{2+}** (M)	**Alk_{tot}** (μM)	pH	**Inst. Rate (mol.m^{-2}.h^{-1})**	**Ω_{ca}**	**SRP** (μM)
G	crystals + NaCl + Phosphate Medium	0	7.24E-07	0	7.88	0	n.a	4.67
		0.016667	1.77E-06	52.6	7.82	5.52E-06	3.64E-05	5.72
		0.083333	6.14E-06	0	7.94	5.75E-06	n.a	6.21
		0.25	1.53E-05	0	7.90	4.82E-06	n.a	6.99
		0.5	3.19E-05	121.5	8.11	5.84E-06	0.0030	6.91
		1	6.79E-05	102.9	8.29	6.32E-06	0.0081	7.69
		6	0.000294	618.2	8.58	3.96E-06	0.399	7.81
		12	0.000410	722.7	8.45	1.70E-06	0.491	7.83
		24	0.000502	896.6	8.59	6.73E-07	1.00	7.99
	PHREEQC		**0.000832**	**5455**	**8.155**		1.00	

Table 3.7: Dissolution Kinetics of Pre-treated Calcite in $\frac{1}{10}$ Phosphate-free Media

Reactor	**Description**	**Time (Hours)**	**Ca^{2+}** (M)	**Alk_{tot}** (μM)	pH	**Inst. Rate** ($mol.m^{-2}.h^{-1}$)	Ω_{ca}	**SRP** (μM)
H	crystals + NaCl + Pre-adsorption + Sample + Phosphate-free Medium	0	6.94E-06	0	6.99	0	n.a	2.55
		0.083333	4.10E-05	76.3	8.21	5.40E-05	0.0030	0.94
		0.25	5.42E-05	0	8.07	6.91E-06	n.a	1.11
		0.5	7.38E-05	135.3	8.09	6.88E-06	0.0073	0.91
		1	0.000105	0	7.94	5.56E-06	n.a	1.07
		5	0.000247	383.8	7.94	3.11E-06	0.049	1.47
		12	0.000421	609.7	8.20	2.18E-06	0.24	1.76
		24	0.000649	896.4	8.23	1.66E-06	0.58	1.79
		72	0.000664	1279	8.30	2.78E-08	1.00	1.67

Table 3.8: Calcite Dissolution Kinetics with Autoclaved Bacteria in $\frac{1}{10}$ Phosphate-limited Media

Reactor	**Description**	**Time (Hours)**	**Ca^{2+}** (M)	**Alk_{tot}** (μM)	pH	**Inst. Rate** (**mol.m^{-2}.h^{-1}**)	**Ω_{ca}**	**SRP** (μM)
I	crystals + NaCl + Autoclaved Sample + Phosphate Medium	0	4.72E-06	n.a	5.79	0	n.a	n.a
		0.083333	2.15E-05	n.a	7.08	2.83E-05	n.a	n.a
		0.25	3.04E-05	66.5	7.09	4.70E-06	0.00015	n.a
		0.5	4.20E-05	n.a	7.21	4.07E-06	n.a	n.a
		1	6.28E-05	90.0	7.38	3.64E-06	0.00082	n.a
		5	0.000179	261.8	7.56	2.56E-06	0.0102	n.a
		12	0.000303	232.3	8.00	1.54E-06	0.042	n.a
		24	0.000517	274.9	8.15	1.56E-06	0.120	n.a
		72	0.000575	1244	8.30	1.08E-07	0.85	n.a

Table 3.9: Calcite Dissolution Kinetics Metabolism Control in $\frac{1}{10}$ Phosphate-limited Media

Reactor	**Description**	**Time (Hours)**	**Ca^{2+}** (M)	**Alk_{tot}** (μ**M**)	pH	**Inst. Rate (mol.m^{-2}.h^{-1})**	**Ω_{ca}**	**SRP** (μ**M**)
J	crystals + NaCl + Sample + Phosphate Medium	0	7.56E-06	n.a	5.74	0	n.a	n.a
		0.083333	3.29E-05	n.a	7.42	5.77E-05	n.a	n.a
		0.25	4.39E-05	94.4	7.45	7.76E-06	0.000704	n.a
		0.5	5.79E-05	n.a	7.50	6.54E-06	n.a	n.a
		1	8.43E-05	109.6	7.60	6.18E-06	0.0022	n.a
		5	0.000203	203.1	7.68	3.46E-06	0.012	n.a
		12	0.000366	525.7	8.00	2.72E-06	0.12	n.a
		24	0.000543	799.0	8.13	1.73E-06	0.35	n.a
		72	0.000604	1287	8.32	1.50E-07	0.95	n.a

presence or absence of phosphate, can be seen in Figure 3.4, where dissolution rates appear fastest in the phosphate-free 0.01M NaCl solution and the phosphate-free growth media. The presence of phosphate, required to sustain bacterial growth in our experiments, strongly inhibits calcite dissolution and masks the effects of bacterial colonisation and metabolism on the dissolution kinetics.

3.4.2.3 Elemental Release Rates (Growth Metabolism)

This set of experiments focussed on qualitative rather than quantitative data analysis, given that sampling volumes were smaller than required for a characterisation of the kinetics. Solutions in these reactors were of a smaller volume (100mL) than in the endogenous metabolism experiments and were sampled only three times in each dissolution cycle/run. Tables 3.10 to 3.18 report calcium concentrations, total alkalinity, pH and instantaneous dissolution rate data as a function of time, for runs in media and in NaCl solutions. Dissolution rates appeared higher in the presence of media, when compared to cycles in NaCl (Figure 3.6). No significant difference in calcium release was seen with consecutive runs in media over time for biotic reactors, whereas a decrease in the amount of calcium released over time was seen in abiotic reactors. Figure 3.5 shows that, in both biotic and abiotic reactors, there was an apparent decrease in the rate of calcium release in the final run in the presence of a 0.01M NaCl solution. There was no significant difference between apparent calcium release rates when pre-treated crystals were exposed to phosphate media and when untreated crystals were immersed in phosphate-containing media (Figure 3.6). Note that in these experiments, a different protocol was adopted from experiments on endogenous metabolism. One possible interpretation is that whether or not the crystals were pre-treated with phosphate, upon phosphate adsorption to the mineral surface (during pre-treatment or upon exposure to the phosphate-containing media), the inhibitory effect was equivalent.

3.4.2.4 Calcite Saturation State (Nutrient-Limited Metabolism)

Dissolution rates under the various experimental conditions were compared on the basis of the saturation state of the experimental solutions (Figure 3.4). The solutions without phosphate generally remained undersaturated with respect to calcite as the rate of

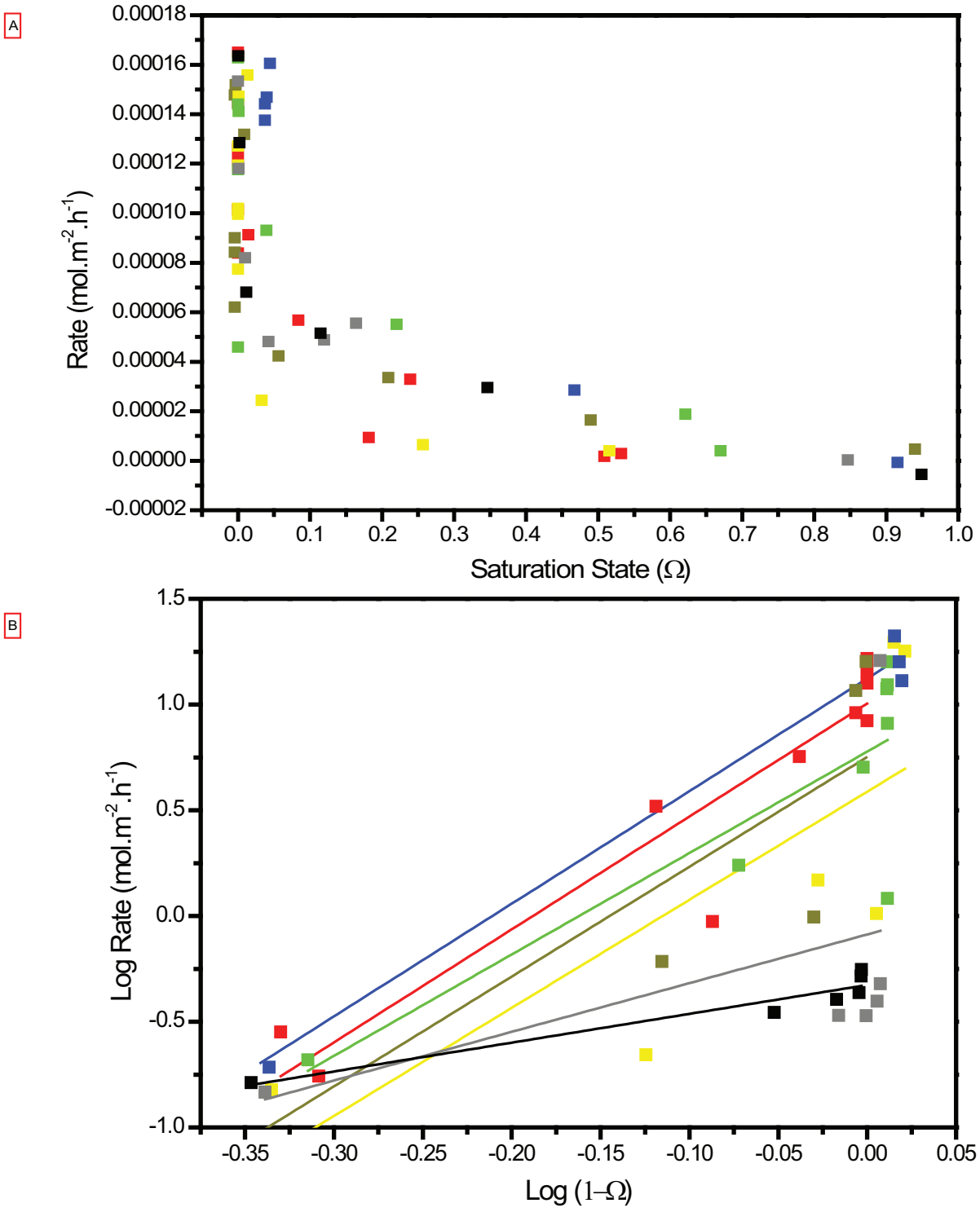

Figure 3.4: (A) Dissolution rates as a function of saturation state, (B) Log rates as a function of log degree of undersaturation, in 0.01M NaCl solution (abiotic (red)), phosphate-free media (abiotic (brown, blue)), phosphate-limited media (abiotic (yellow, green)), batch experiment with autoclaved bacteria in phosphate media (grey) and bacterial metabolic control experiment in phosphate media (black).

Table 3.10: Calcite dissolution trends of phosphate-treated calcite in $\frac{1}{10}$ phosphate-free media

Reactor	**Description**	**Time (Hours)**	**Ca^{2+}** (M)	**Alk_{tot} (μM)**	pH	**Inst. Rate (mol.m^{-2}.h^{-1})**	**Ω_{ca}**	**SRP (μM)**
K1	crystals + NaCl + Sample + Phosphate-free Medium	0	3.24E-07	n.a	6.23	0	n.a	n.a
		5	0.000232	745.9	7.98	0.00116	0.099	n.a
		48	0.000397	1319	8.24	9.57E-05	0.54	n.a
		0	1.05E-06	n.a	6.25	0	n.a	n.a
		5	0.00026	658.5	7.92	0.00130	0.085	n.a
		48	0.000498	1378	8.18	0.000138	0.62	n.a
		0	6.49E-07	n.a	6.12	0	n.a	n.a
		5	0.000218	568.3	7.79	0.00109	0.046	n.a
		48	0.00047	1328	8.02	0.000146	0.39	n.a
		0	7.49E-07	n.a	6.08	0	n.a	n.a
		5	0.000172	n.a	7.70	0.000857	0.00	n.a
		48	0.000662	1176	8.15	0.000285	0.65	n.a
	crystals + NaCl + Water	(R5) 0	1.37E-06	n.a	6.13	0	n.a	n.a
		5	9.94E-05	194.9	7.40	0.00049	0.003	n.a
		48	0.00034	732.4	8.00	0.00014	0.15	n.a

Table 3.11: Calcite dissolution rates for phosphate-treated calcite in $\frac{1}{10}$ phosphate-free media

Reactor	**Description**	**Time (Hours)**	**Ca^{2+}** (M)	**Alk_{tot} (μM)**	pH	**Inst. Rate ($mol.m^{-2}.h^{-1}$)**	**Ω_{ca}**	**SRP (μM)**
K2	crystals + NaCl + Sample + Phosphate Free Medium	0	8.98E-07	n.a	6.01	0	n.a	n.a
		5	0.000228	755.4	7.94	0.00113	0.090	n.a
		48	0.000424	1271	8.25	0.000114	0.57	n.a
		0	7.49E-07	n.a	6.11	0	n.a	n.a
		5	0.00028	675.1	7.98	0.00140	0.11	n.a
		48	0.000513	1458	8.24	0.000136	0.78	n.a
		0	9.98E-08	n.a	6.09	0	n.a	n.a
		5	0.000246	713.3	7.47	0.00123	0.031	n.a
		48	0.000514	1383	8.18	0.000156	0.64	n.a
		0	7.73E-07	n.a	6.02	0	n.a	n.a
		5	0.000203	n.a	7.81	0.00101	0.00	n.a
		48	0.000684	1242	8.18	0.00028	0.77	n.a
	crystals + NaCl + Water	(R5) 0	1.42E-06	n.a	5.891	0	n.a	n.a
		5	0.000138	193.5	7.56	0.000682	0.006	n.a
		48	0.000422	849.6	8.02	0.000165	0.23	n.a

Table 3.12: Calcite dissolution rates for phosphate-treated calcite in $\frac{1}{10}$ phosphate-free media

Reactor	**Description**	**Time (Hours)**	**Ca^{2+}** (M)	**Alk_{tot}** (μM)	pH	**Inst. Rate (mol.m^{-2}.h^{-1})**	**Ω_{ca}**	**SRP** (μM)
K3	crystals + NaCl + Sample + Phosphate Free Medium	0	9.73E-07	n.a	5.96	0	n.a	1.16
		5	0.000255	668.5	8.01	0.00127	0.103	7.07
		48	0.000429	1483	8.22	0.000102	0.62	15.1
		0	4.74E-07	n.a	6.07	0	n.a	0.55
		5	0.000284	694.0	7.98	0.00142	0.11	4.68
		48	0.000524	1535	8.28	0.00014	0.89	8.89
		0	3.74E-07	n.a	6.08	0	n.a	0.158
		5	0.000249	626.9	7.75	0.00125	0.052	3.18
		48	0.000526	1543	8.14	0.000161	0.66	4.61
		0	3.49E-07	n.a	6.01	0	n.a	0.104
		5	0.000194	516.6	7.84	0.000966	0.041	2.22
		48	0.000713	1311	8.14	0.000302	0.77	5.19
	crystals (5g) + 0.01g NaCl + Sample + Water (100mL)	(R5) 0	1.52E-06	n.a	5.89	0	n.a	0.216
		5	0.000137	208.8	7.50	0.000678	0.005	3.22
		48	0.00033	849.2	7.88	0.000112	0.13	7.06

Table 3.13: Calcite dissolution rates of calcite in the presence of autoclaved bacteria in $\frac{1}{10}$ phosphate-limited media

Reactor	**Description**	**Time (Hours)**	**Ca^{2+}** (M)	**Alk_{tot}** (μM)	pH	**Inst. Rate** (**mol.m^{-2}.h^{-1}**)	**Ω_{ca}**	**SRP** (μM)
L1	crystals + NaCl + Autoclaved Sample + Phosphate Limited Medium	0	0	n.a	6.36	0	n.a	n.a
		5	0.000566	n.a	7.74	0.00283	0	n.a
		48	0.000872	914.3	8.09	0.000178	0.58	n.a
		0	8.48E-07	n.a	6.31	0	n.a	n.a
		5	0.000298	n.a	7.87	0.00149	0	n.a
		48	0.000535	1308	8.04	0.000138	0.45	n.a
		0	0	n.a	6.13	0	n.a	n.a
		5	0.000229	n.a	7.71	0.00114	0	n.a
		48	0.000517	1268	8.05	0.000168	0.44	n.a
		0	4.49E-07	n.a	6.17	0	n.a	n.a
		5	0.000213	515.8	7.70	0.00106	0.033	n.a
		48	0.000479	1151	8.09	0.000155	0.41	n.a
	crystals (5g) + 0.01g NaCl + Autoclaved Sample + Water (100mL)	0	5.99E-07	n.a	5.93	0	n.a	n.a
		5	0.000114	306.3	5.57	0.000565	0.00	n.a
		48	0.00033	778.1	8.00	0.000126	0.15	n.a

Table 3.14: Calcite dissolution rates of calcite in the presence of autoclaved bacteria in $\frac{1}{10}$ phosphate-limited media

Reactor	**Description**	**Time (Hours)**	**Ca^{2+}** (M)	**Alk_{tot}** (μM)	pH	**Inst. Rate** (**$mol.m^{-2}.h^{-1}$**)	**Ω_{ca}**	**SRP** (μM)
L2	crystals (5g) + 0.01g NaCl + Autoclaved Sample + Phosphate Limited Medium (100mL)	0	0	n.a	6.20	0	n.a	n.a
		5	0.000479	449.0	7.82	0.00240	0.085	n.a
		48	0.000822	1216	8.15	0.000199	0.83	n.a
		0	1.02E-06	n.a	6.32	0	n.a	n.a
		5	0.000335	820.7	7.90	0.00167	0.13	n.a
		48	0.000546	1442	7.89	0.000122	0.36	n.a
		0	0	n.a	6.10	0	n.a	n.a
		5	0.000245	0	7.72	0.00123	0	n.a
		48	0.000552	1332	7.98	0.000178	0.41	n.a
		0	7.98E-07	n.a	6.06	0	n.a	n.a
		5	0.000262	0	7.8	0.00131	0	n.a
		48	0.000521	1174	8.13	0.000151	0.49	n.a
	crystals (5g) + 0.01g NaCl + Autoclaved Sample + Water (100mL)	0	4.99E-07	n.a	5.82	0	n.a	n.a
		5	0.000152	376.2	7.43	0.000755	0.009	n.a
		48	0.000411	924.4	8.08	0.000151	0.27	n.a

Table 3.15: Calcite dissolution rates of calcite in the presence of autoclaved bacteria in $\frac{1}{10}$ phosphate-limited media

Reactor	**Description**	**Time (Hours)**	**Ca^{2+}** (M)	**Alk_{tot}** (μM)	pH	**Inst. Rate (mol.m^{-2}.h^{-1})**	**Ω_{ca}**	**SRP** (μM)
L3	crystals (5g) + 0.01g NaCl + Autoclaved Sample + Phosphate Limited Medium (100mL)	0	4.99E-07	n.a	6.19	0	n.a	7.30
		5	0.000543	487.3	7.75	0.00271	0.088	7.00
		48	0.000832	1033	8.11	0.000168	0.65	8.43
		0	5.49E-07	n.a	6.25	0	n.a	7.06
		5	0.000286	636.0	7.97	0.00143	0.10	11.0
		48	0.000494	1266	8.087	0.000121	0.45	11.1
		0	9.98E-08	n.a	6.08	0	n.a	7.10
		5	0.000299	700.1	7.78	0.00149	0.075	12.7
		48	0.000535	1284	8.13	0.000138	0.55	13.1
		0	1.07E-06	n.a	6.05	0	n.a	6.87
		5	0.000241	572.3	7.82	0.00120	0.054	8.90
		48	0.00052	1207	8.11	0.000163	0.48	10.5
	crystals (5g) + 0.01g NaCl + Autoclaved Sample + Water (100mL)	0	1.25E-06	n.a	5.77	0	n.a	0.068
		5	0.00012	297.8	7.69	0.000595	0.010	6.65
		48	0.000383	858.2	8.01	0.000153	0.20	7.33

Table 3.16: Calcite dissolution rates of calcite in $\frac{1}{10}$ phosphate-limited media

Reactor	**Description**	**Time (Hours)**	**Ca^{2+}** (M)	**Alk_{tot}** (μM)	pH	**Inst. Rate (mol.m^{-2}.h^{-1})**	**Ω_{ca}**	**SRP** (μM)
M1	crystals (5g) + 0.01g NaCl + Sample + Phosphate Limited Medium (100mL)	0	0	n.a	6.41	0	n.a	n.a
		5	0.000268	784.7	8.03	0.00134	0.13	n.a
		48	0.000458	1314	8.26	0.00011	0.64	n.a
		0	4.74E-07	n.a	6.38	0	n.a	n.a
		5	0.000223	555.7	7.88	0.00111	0.056	n.a
		48	0.00049	1226	8.14	0.000155	0.49	n.a
		0	0	n.a	6.24	0	n.a	n.a
		5	0.000205	509.4	7.64	0.00103	0.028	n.a
		48	0.000489	1195	8.03	0.000165	0.38	n.a
		0	5.74E-07	n.a	6.13	0	n.a	n.a
		5	0.000209	0	7.71	0.00105	0.00	n.a
		48	0.000456	1127	8.06	0.000143	0.35	n.a
	crystals (5g) + 0.01g NaCl + Sample + Water (100mL)	0	1.85E-06	n.a	6.15	0	n.a	n.a
		5	0.000139	204.5	7.44	0.000684	0.005	n.a
		48	0.000351	758.3	7.80	0.000124	0.10	n.a

Table 3.17: Calcite dissolution rates of calcite in $\frac{1}{10}$ phosphate-limited media

Reactor	**Description**	**Time (Hours)**	**Ca^{2+}** (M)	**Alk_{tot}** (μM)	pH	**Inst. Rate (mol.m^{-2}.h^{-1})**	**Ω_{ca}**	**SRP** (μM)
M2	crystals (5g) + 0.01g NaCl + Sample + Phosphate Limited Medium (100mL)	0	0	n.a	6.25	0	n.a	n.a
		5	0.000245	766.6	7.99	0.00123	0.109	n.a
		48	0.00047	1390	8.28	0.000131	0.740	n.a
		0	3.99E-07	n.a	6.31	0	n.a	n.a
		5	0.000303	745.5	8.04	0.00152	0.147	n.a
		48	0.00054	1362	8.19	0.000138	0.677	n.a
		0	0	n.a	6.11	0	n.a	n.a
		5	0.000255	649.2	7.68	0.00128	0.047	n.a
		48	0.00053	1330	8.06	0.00016	0.480	n.a
		0	6.99E-07	n.a	6.04	0	n.a	n.a
		5	0.000268	0	7.79	0.00134	0	n.a
		48	0.000465	1206	8.13	0.000114	0.445	n.a
	crystals (5g) + 0.01g NaCl + Sample + Water (100mL)	0	2.12E-06	n.a	5.84	0	n.a	n.a
		5	0.000136	0	7.51	0.000671	0	n.a
		48	0.000407	810.9	7.92	0.000158	0.162	n.a

Table 3.18: Calcite dissolution rates of calcite in $\frac{1}{10}$ phosphate-limited media

Reactor	**Description**	**Time (Hours)**	**Ca^{2+}** (M)	**Alk_{tot}** (μM)	pH	**Inst. Rate** ($mol.m^{-2}.h^{-1}$)	**Ω_{ca}**	**SRP** (μM)
M3	crystals (5g) + 0.01g NaCl + Sample + Phosphate Limited Medium (100mL)	0	3.74E-07	n.a	6.23	0	n.a	7.19
		5	0.000246	646.6	7.97	0.00123	0.088	10.8
		48	0.000459	1309	8.23	0.000124	0.602	14.1
		0	0	n.a	6.26	0	n.a	7.40
		5	0.000254	645.0	7.95	0.00127	0.087	10.9
		48	0.00049	1285	8.12	0.000137	0.494	12.9
		0	0	n.a	6.09	0	n.a	10.8
		5	0.000242	656.4	7.56	0.00121	0.035	10.9
		48	0.000515	1314	8.00	0.000159	0.401	14.8
		0	3.24E-07	n.a	6.02	0	n.a	6.89
		5	0.000243	0	7.70	0.00121	0	12.9
		48	0.000476	1211	8.22	0.000136	0.566	9.58
	crystals (5g) + 0.01g NaCl + Sample + Water (100mL)	0	2.15E-06	n.a	5.83	0	n.a	0
		5	0.000153	0	7.66	0.000757	0	5.29
		48	0.000613	825.3	7.95	0.000267	0.270	14.2

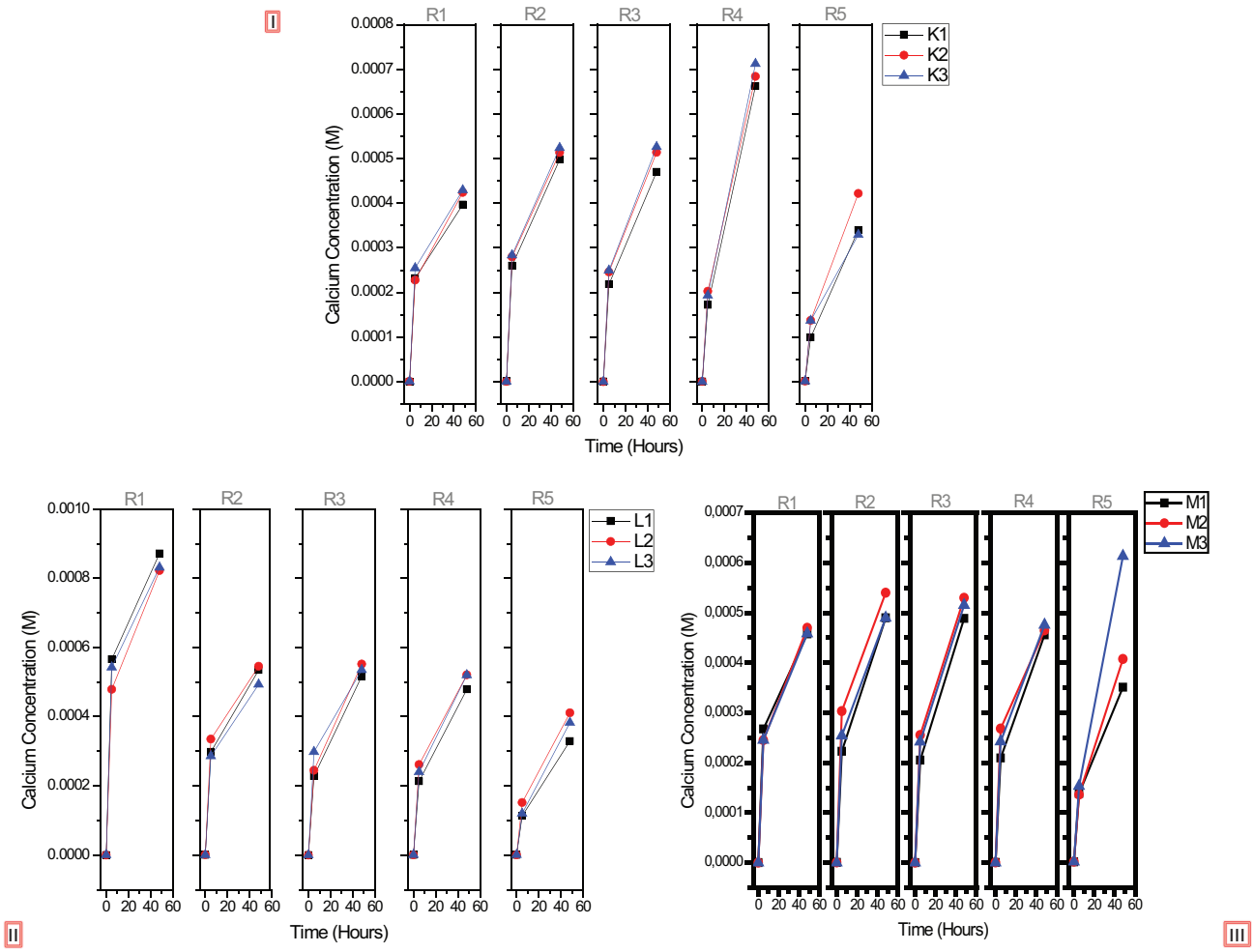

Figure 3.5: Temporal evolution of calcium concentrations during calcite dissolution in media (R1-R4) and in 0.01M NaCl solutions (R5), in separate reactors: K, L and M. Batch experiments with pre-treated calcite crystals and phosphate-free media (I), batch experiments with autoclaved bacteria in phosphate media (II) and bacterial metabolic control experiments in phosphate media (III). K1-M3 are reactor replicates, listed in Tables 3.10 to 3.18.

dissolution approached zero. Solutions in biotic reactors were undersaturated with respect to calcite for the duration of experiments. When fit to the logarithmic form of equation 3.3, the data generally yield coefficients of determination (R^2) between 0.67 and 0.98 for both biotic and abiotic reactors (Figure 3.4(B)).

3.4.2.5 Calcite Saturation State (Growth Metabolism)

Upon immersion of the calcite crystals, media solutions approached saturation more quickly than in NaCl solutions (Figure 3.6) and all solutions remained undersaturated with respect to calcite throughout the experiments. Solutions containing phosphate pre-treated calcite approached saturation more readily in comparison to non-treated calcite crystals in phosphate media. Solutions with autoclaved bacteria remained more undersaturated with respect to calcite as dissolution rates approached zero, in comparison to reactors with phosphate media and viable bacteria. These data could not be fit to the empirical dissolution rate function (eq. 3.3) or its logarithmic form.

3.4.2.6 Influence of Phosphate (Nutrient-Limited Metabolism)

The SRP was measured in abiotic and biotic reactors to investigate the inhibitory effect on calcite dissolution. Phosphate can complex with lattice calcium ions at high energy sites (typically steps and kinks), at the surface of the mineral, inhibiting the rate of dissolution [22, 27, 32]. The inhibitory efficiency of phosphate increases as saturation is approached [28]. The calcium release rate was seen to decrease more rapidly in reactors containing phosphate (E, G) in comparison to phosphate-free reactors (D, F) at similar saturation states (see Figure 3.4).

As seen in Figure 3.8, for reactors with phoshate pre-treated calcite, in the presence of bacteria, the SRP concentration decreased rapidly within the first 5 minutes of reaction and then became nearly constant over time. This may be interpreted as the assimilation of SRP by bacteria to sustain their growth and metabolism. The SRP concentration appeared to increase over time in the absence of bacteria, comparable to observations by Wu and Jacobson (2009) [22]. This may reflect the desorption of adsorbed SRP from the pre-treated calcite crystal.

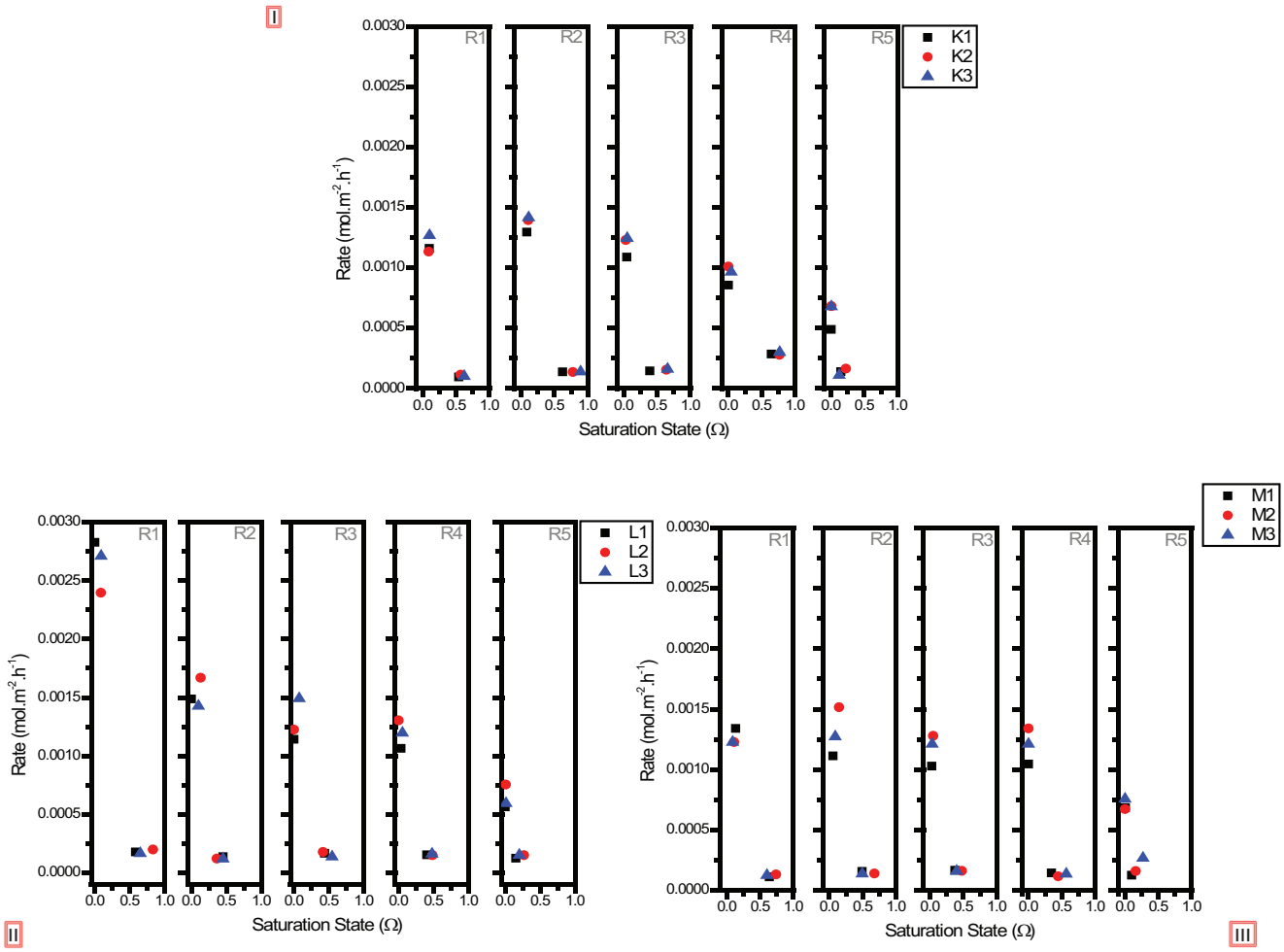

Figure 3.6: Dissolution rates as a function of saturation state in media (R1-R4) and in 0.01M NaCl solutions (R5), in separate reactors K, L and M. Batch experiments with pre-treated calcite and phosphate-free media (I), batch experiment with autoclaved bacteria in phosphate media (II) and bacterial metabolic control experiment in phosphate media (III). K1-M3 are reactor replicates, listed in Tables 3.10 to 3.18.

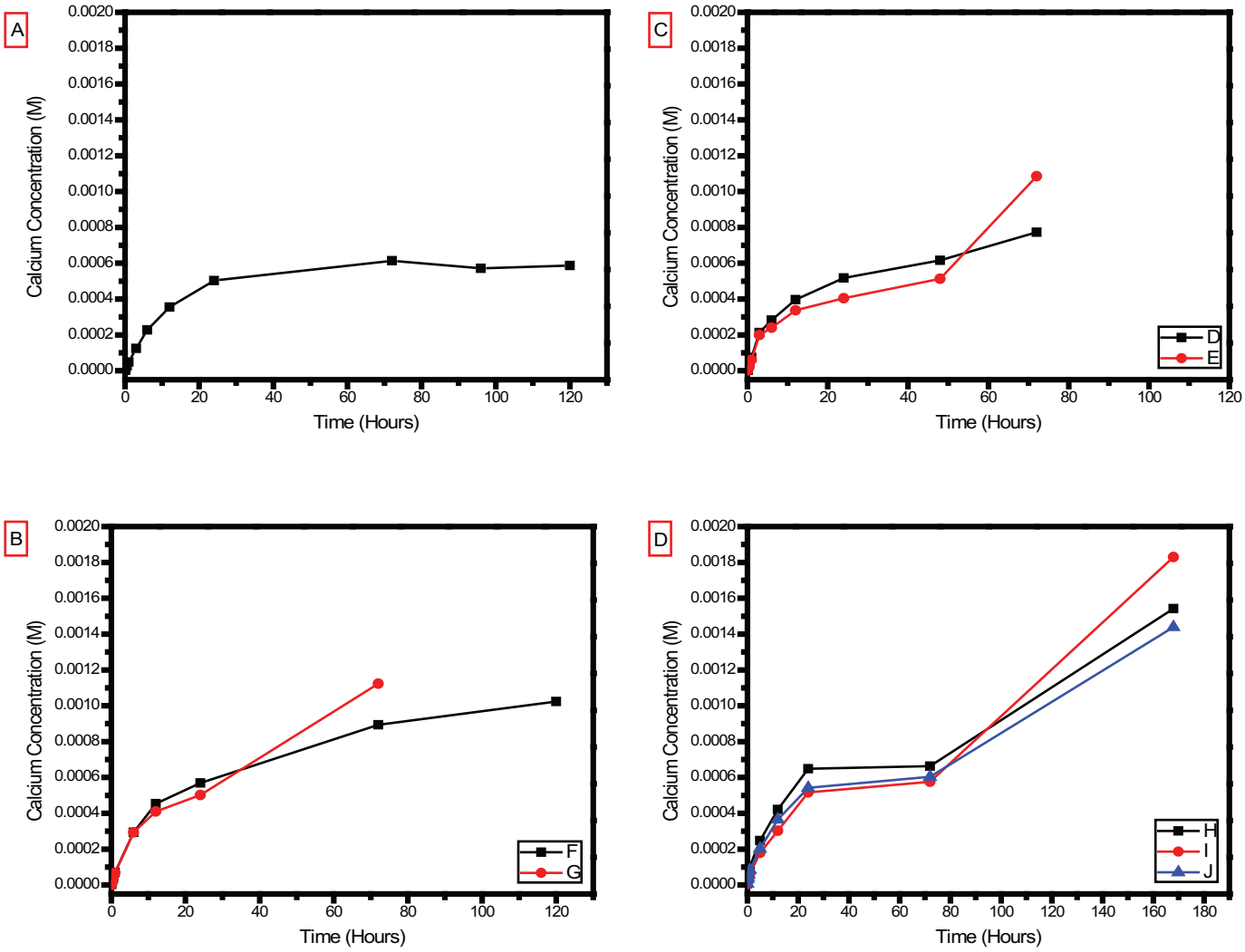

Figure 3.7: (A) Temporal evolution of calcium concentration during calcite dissolution in 0.01M NaCl solutions (reactor I). (B and C) Abiotic phosphate-free media (reactors D, F) vs. abiotic phosphate-limited media (reactors E, G). (D) Batch experiment with pre-treated calcite (reactor H), batch experiment with autoclaved bacteria (reactor I) and bacterial metabolic control experiment (reactor J).

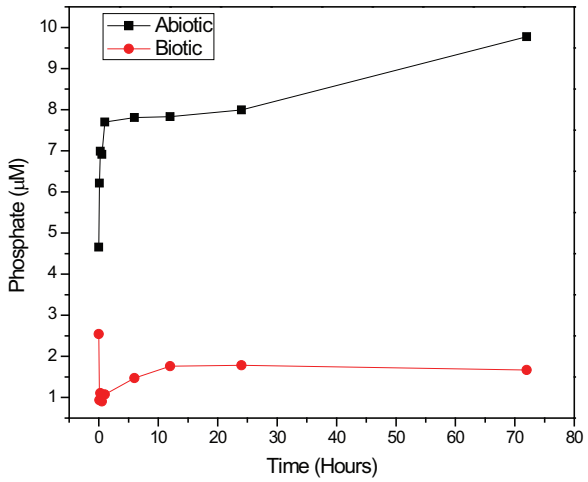

Figure 3.8: Temporal evolution of dissolved phosphate (SRP) during calcite dissolution experiments in abiotic phosphate-limited media (G) and biotic batch experiments with pre-treated calcite (H).

3.4.2.7 Influence of Phosphate (Growth Metabolism)

There was up to twice the SRP concentration in reactors with phosphate-containing media than in reactors with pre-treated crystals (Tables 3.12, 3.15 and 3.18). As expected, in dissolution experiments with the greater SRP concentration, the amount of calcium released into solution over time was less than in experiments with SRP pre-treated crystals. In other words, at greater SRP concentrations there is greater calcite dissolution inhibition and calcium concentrations are lower.

3.4.2.8 Bacterial Attachment (Nutrient-Limited Metabolism)

Varying degrees of bacterial coverage on crystals surfaces was observed using light microscopy. Figure 3.9 illustrates the main observations, ranging from homogeneous to patchy and fine to more coarse-grained surfaces. The degree of bacterial coverage of the crystal surfaces was correlated with the density of cell-like structures observed upon staining and fluorescence microscopy. Homogeneous 'granular' coverage revealed more

Figure 3.9: Degrees of bacterial coverage. Pristine vs. colonised crystal surfaces (10× magnification). Clockwise from top-left: pristine calcite rhomb, granular deposition upon incubation with weathered samples; greater deposition of weathered material along steps or in troughs; flatter crystal profiles showing more homogeneous coverage by weathered material and thus, by bacteria.

definite cell-like structures, whereas patchy coverage most often showed 'filmy' or 'cloudy' structures at the crystal surface (Figures 3.10 (II, V) and (III, VI)).

3.4.2.9 Bacterial Attachment (Growth Metabolism)

Structures on crystal surfaces exposed to viable bacteria in the presence of phosphate media were more visible than on phosphate-treated crystals (Figures 3.11 to 3.13). In the former, fluorescence microscopy showed greater densities of cell-like structures and the presence of linkages which resemble biofilms. In one set of reactors containing autoclaved weathered samples, fluorescence microscopy revealed a homogeneous coverage of the crystal surface by bacteria-like cell structures (Figure 3.12 (II)). Nevertheless, since cell-like structures were absent from replicate surfaces and given that these cells appeared identical in morphology, this observation is interpreted as the colonisation of a

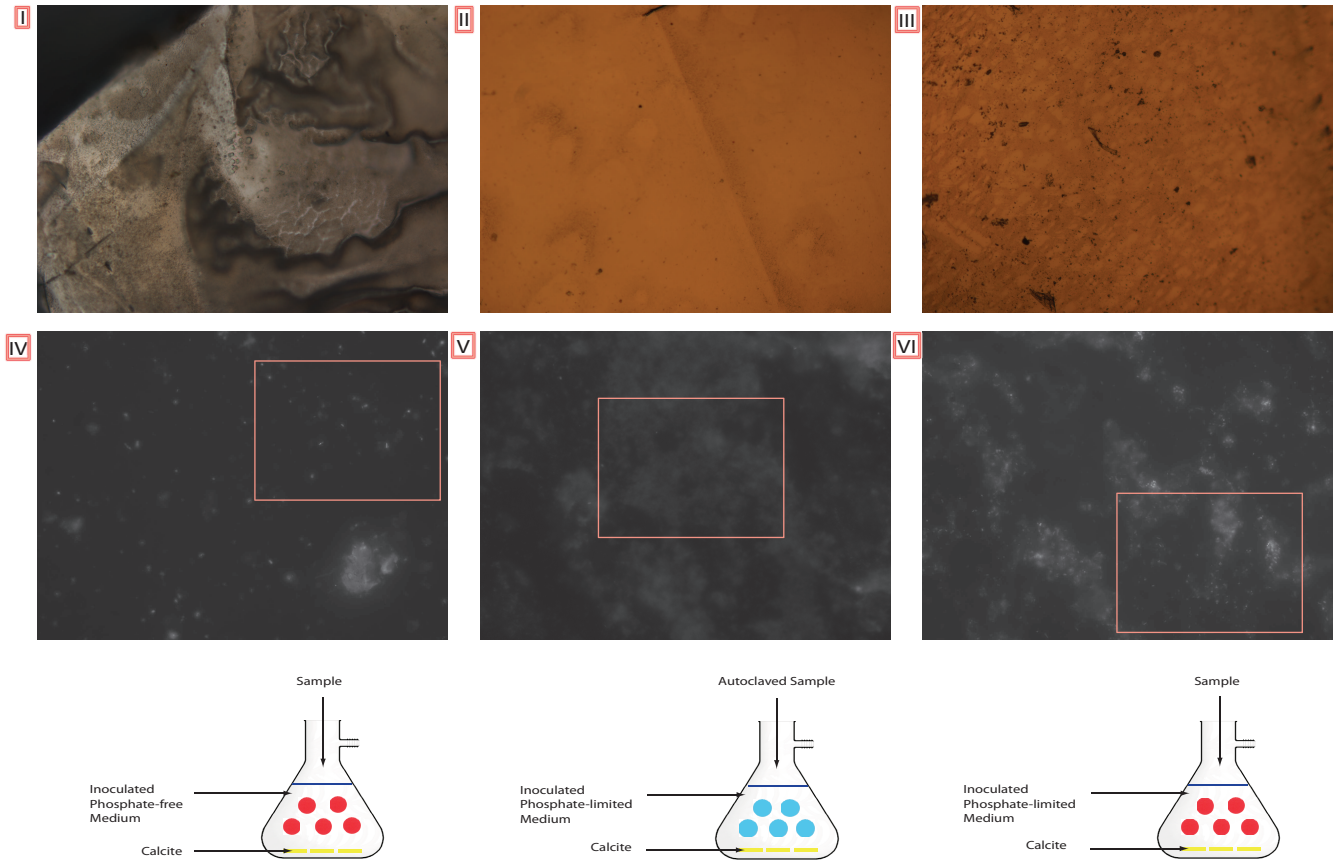

Figure 3.10: Bacterial coverage of crystal surfaces following batch experiments. Bright Field, 10× magnification (I-III); DAPI stain with fluorescence microscopy, 60× (IV-VI).

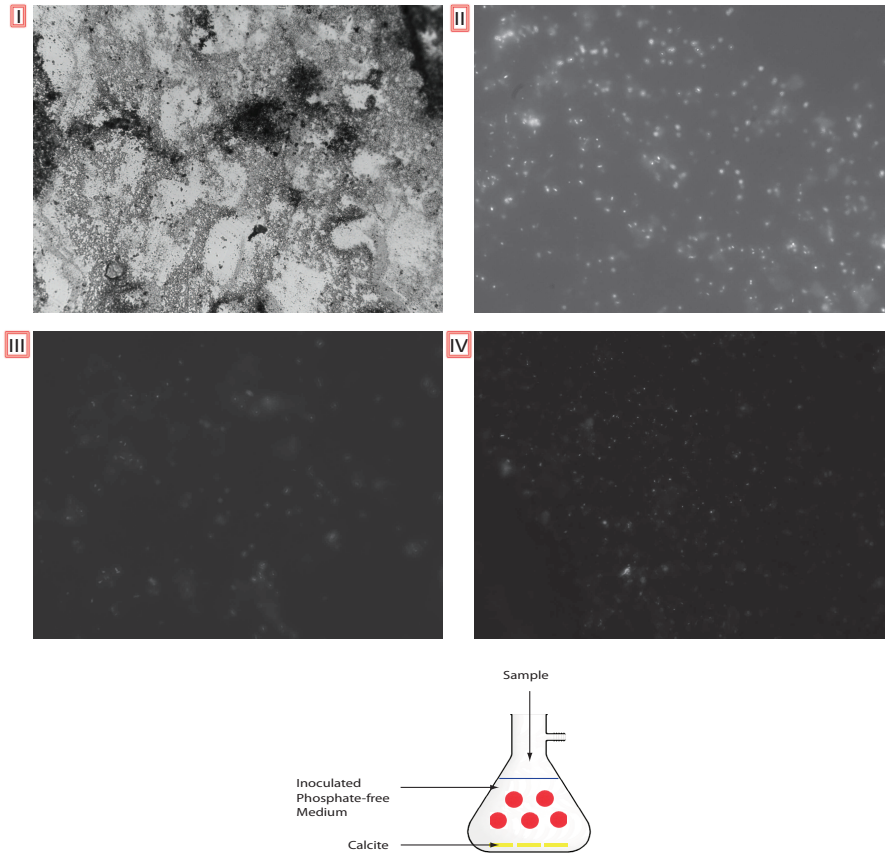

Figure 3.11: Bacterial coverage of pre-treated crystal surfaces in (Growth Metabolism) batch experiments. Crystal in medium, Bright Field 10× magnification (I); crystal in medium, DAPI 100× (II, III); crystal in NaCl solution, DAPI 65× (IV).

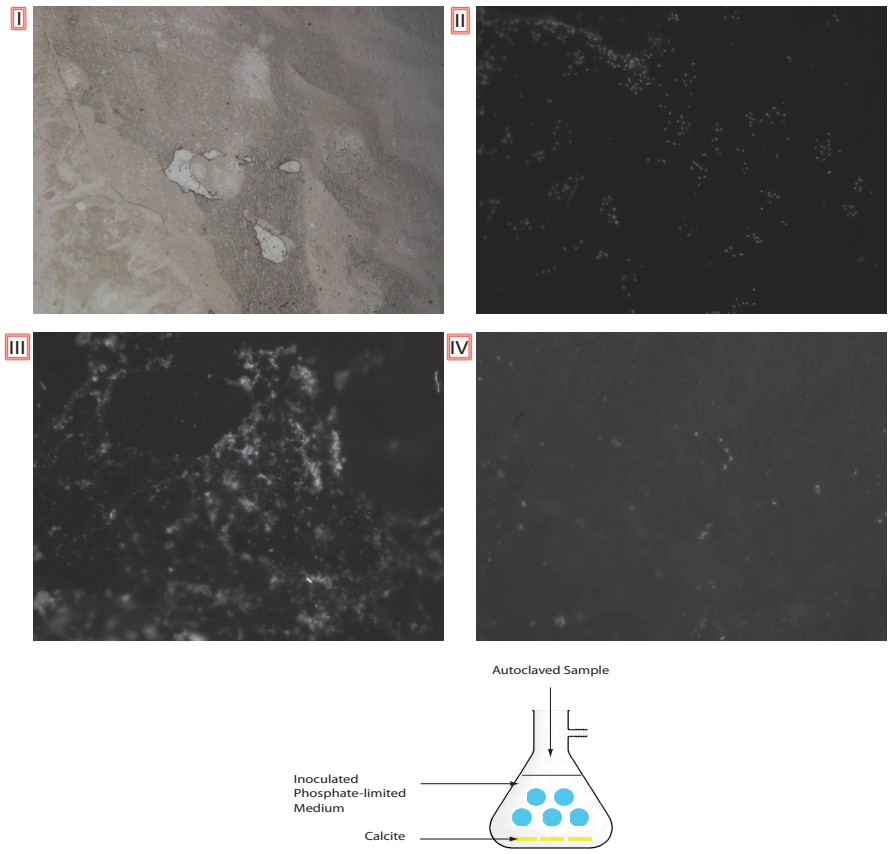

Figure 3.12: Bacterial coverage of crystal surfaces exposed to autoclaved weathered samples in the presence of phosphate media. Crystal in medium, Bright Field 10× magnification (I); crystal in medium, DAPI 65× with apparent bacterial contamination (II) and without contamination (III); crystal in NaCl solution, DAPI 65× (IV).

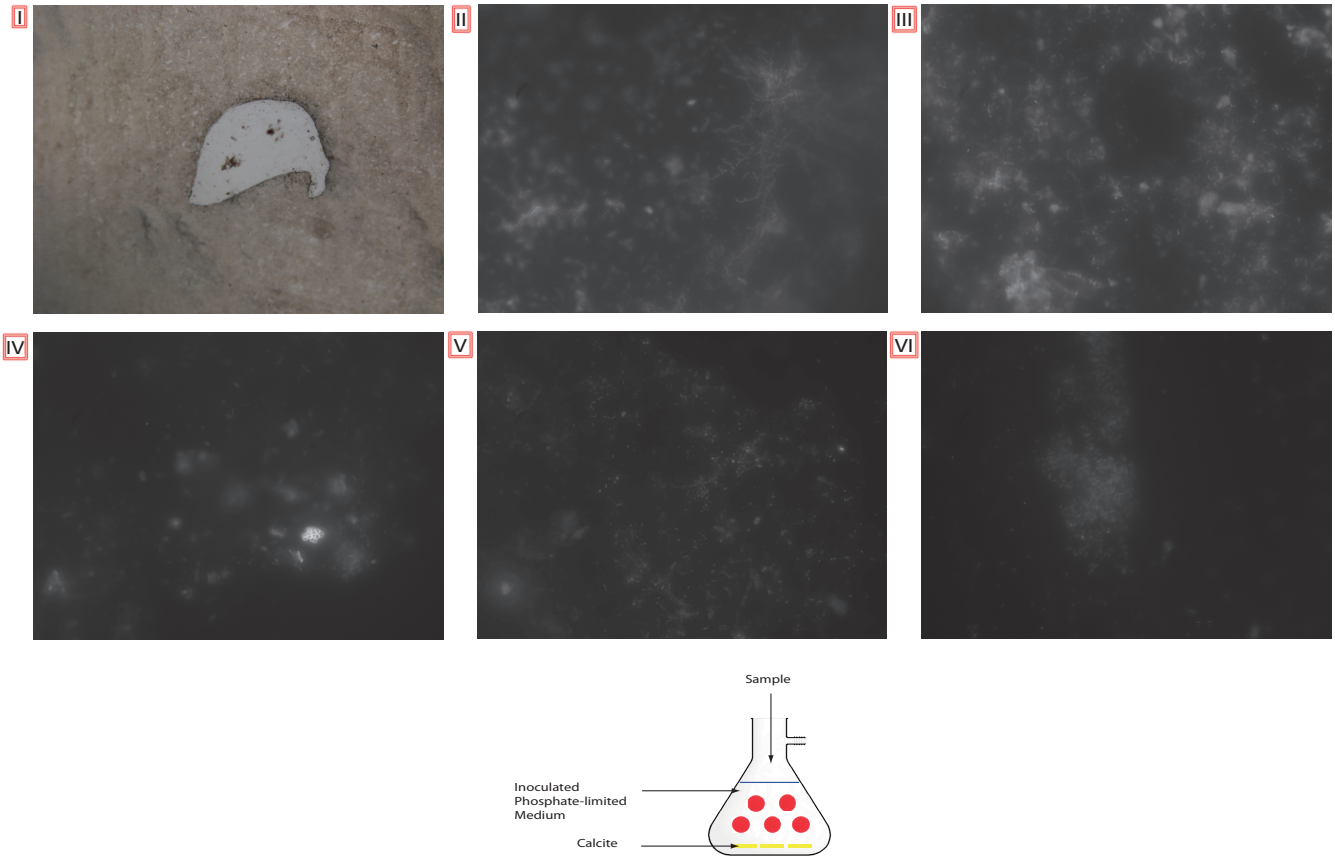

Figure 3.13: Bacterial coverage of crystal surfaces following batch experiments with viable bacteria in phosphate media. Crystal in medium, Bright Field 10× (I); crystal in medium, DAPI 100× (II-V); crystal in NaCl solution, DAPI 100× (VI).

single predominant species whose presence is most likely attributed to contamination. It is important to note that, after introducing the crystals into saline solutions following exposure to the media, definite cell-like structures were still observed on crystal surfaces from reactors inoculated with viable weathered samples, but these were no longer noticeable on (contaminated) crystals in reactors inoculated with autoclaved samples (Figure 3.12 (IV)).

The bacterial agglomerations on crystal surfaces in reactors inoculated with viable weathered samples comprise cells with slight morphological variations, suggesting that they are collections of several strains. The relative abundance of cells in reactors with phosphate media is interpretable from the relative SRP concentrations, as seen in Tables 3.12, 3.15 and 3.18. In reactors with pre-treated crystals, most phosphate is bound to the surface and thus, not as much is freely available in solution for the bacteria. This would explain the greater amount of colonisation of crystals exposed to phosphate media. This indicates that bacterial colonisation is nutrient-limited in the case of phosphate-treated calcite crystals.

3.5 Conclusion

Experiments conducted in the presence and absence of phosphate and/or bacteria indicate that calcite dissolution is inhibited in the presence of bacteria and freely-available phosphate. Reduced rates of dissolution and greater degrees of surface colonisation were observed in growth media containing phosphate. At greater SRP concentrations, there is greater calcite dissolution inhibition and the amount of calcium released in solution was reduced.

3.6 Acknowledgements

Funding for research was provided by the Natural Sciences and Engineering Research Council of Canada (NSERC), through grants to Alfonso Mucci. We thank Constance Guignard for technical assistance, Glenna Keating and Isabelle Richer for XRF and

assistance with AAS; Jean-François Hélie and Agnieszka Adamowicz for total Carbon and Nitrogen analyses; Michel Préda for XRD.

Bibliography

[1] L. Wu, A. D. Jacobson, and M. Hausner, "Characterization of elemental release during microbe-granite interactions at T=28 °C," *Geochimica et Cosmochimica Acta*, vol. 72, no. 4, pp. 1076–1095, 2008.

[2] H. L. Ehrlich, "Geomicrobiology: its significance for geology," *Earth-Science Reviews*, vol. 45, no. 1-2, pp. 45–60, 1998.

[3] W. W. Barker and J. F. Banfield, "Zones of chemical and physical interaction at interfaces between microbial communities and minerals: A model," *Geomicrobiology Journal*, vol. 15, no. 3, pp. 223 – 244, 1998.

[4] W. J. Ullman, D. L. Kirchman, S. A. Welch, and P. Vandevivere, "Laboratory evidence for microbially mediated silicate mineral dissolution in nature," *Chemical Geology*, vol. 132, no. 1-4, pp. 11–17, 1996.

[5] S. A. Welch, W. W. Barker, and J. F. Banfield, "Microbial extracellular polysaccharides and plagioclase dissolution," *Geochimica et Cosmochimica Acta*, vol. 63, no. 9, pp. 1405–1419, 1999.

[6] N. H. de Leeuw and S. C. Parker, "Surface structure and morphology of calcium carbonate polymorphs calcite, aragonite, and vaterite: An atomistic approach," *The Journal of Physical Chemistry B*, vol. 102, no. 16, pp. 2914–2922, 1998.

[7] M. Rivadeneyra, I. Perez-Garcia, V. Salmeron, and A. Ramos-Cormenzana, "Bacterial precipitation of calcium carbonate in presence of phosphate," *Soil Biology and Biochemistry*, vol. 17, no. 2, pp. 171 – 172, 1985.

[8] F. Ferris, V. Phoenix, Y. Fujita, and R. Smith, "Kinetics of calcite precipitation induced by ureolytic bacteria at 10 to 20c in artificial groundwater," *Geochimica et Cosmochimica Acta*, vol. 68, no. 8, pp. 1701 – 1710, 2004.

[9] D. V. Zamarreño, R. Inkpen, and E. May, "Carbonate crystals precipitated by freshwater bacteria and their use as a limestone consolidant," *Appl. Environ. Microbiol.*, vol. 75, no. 18, pp. 5981–5990, 2009.

[10] J. T. DeJong, B. M. Mortensen, B. C. Martinez, and D. C. Nelson, "Bio-mediated soil improvement," *Ecological Engineering*, vol. 36, no. 2, pp. 197 – 210, 2010. Special Issue: BioGeoCivil Engineering.

[11] A. L*ü*ttge and P. G. Conrad, "Direct observation of microbial inhibition of calcite dissolution," *Applied and Environmental Microbiology*, vol. 70, no. 3, pp. 1627–1632, 2004.

[12] C. M. Santelli, S. A. Welch, H. R. Westrich, and J. F. Banfield, "The effect of fe-oxidizing bacteria on fe-silicate mineral dissolution," *Chemical Geology*, vol. 180, no. 1-4, pp. 99–115, 2001.

[13] S. A. Welch, A. E. Taunton, and J. F. Banfield, "Effect of microorganisms and microbial metabolites on apatite dissolution," *Geomicrobiology Journal*, vol. 19, no. 3, pp. 343–367, 2002.

[14] A. K. Friis, T. A. Davis, M. M. Figueira, J. Paquette, and A. Mucci, "Influence of bacillus subtilis cell walls and EDTA on calcite dissolution rates and crystal surface features," *Environmental Science and Technology*, vol. 37, no. 11, pp. 2376– 2382, 2003.

[15] A. L*ü*ttge, L. Zhang, and K. H. Nealson, "Mineral surfaces and their implications for microbial attachment: Results from monte carlo simulations and direct surface observations," *American Journal of Science*, vol. 305, pp. 766– 790, 2005.

[16] H. L. Buss, A. L*ü*ttge, and S. L. Brantley, "Etch pit formation on iron silicate surfaces during siderophore-promoted dissolution," *Chemical Geology*, vol. 240, no. 3-4, pp. 326–342, 2007.

[17] R. G. Arnold, T. J. DiChristina, and M. R. Hoffmann, "Reductive dissolution of Fe(iii) oxides by Pseudomonas sp. 200," *Biotechnology and Bioengineering*, vol. 32, no. 9, pp. 1081–1096, 1988.

[18] P. Vandevivere, S. A. Welch, W. J. Ullman, and D. L. Kirchman, "Enhanced dissolution of silicate minerals by bacteria at near-neutral ph," *Microbial Ecology*, vol. 27, pp. 241–251, 1994.

[19] L. Hersman, T. Lloyd, and G. Sposito, "Siderophore-promoted dissolution of hematite," *Geochimica et Cosmochimica Acta*, vol. 59, no. 16, pp. 3327–3330, 1995.

[20] L. J. Liermann, B. E. Kalinowski, S. L. Brantley, and J. G. Ferry, "Role of bacterial siderophores in dissolution of hornblende," *Geochimica et Cosmochimica Acta*, vol. 64, no. 4, pp. 587–602, 2000.

[21] K. J. Davis, K. H. Nealson, and A. Lüttge, "Calcite and dolomite dissolution rates in the context of microbe-mineral surface interactions," *Geobiology*, vol. 5, no. 2, pp. 191–205, 2007.

[22] D. Jacobson, Andrew and L. Wu, "Microbial dissolution of calcite at T = 28 °C and ambient pCO_2," *Geochimica et Cosmochimica Acta*, vol. 73, pp. 2314–2331, 2009.

[23] I. Clarridge, Jill E., "Impact of 16s rrna gene sequence analysis for identification of bacteria on clinical microbiology and infectious diseases," *Clin. Microbiol. Rev.*, vol. 17, no. 4, pp. 840–862, 2004.

[24] N. E. Pingitore, S. B. Fretzdorff, B. P. Seitz, L. Y. Estrada, P. M. Borrego, G. M. Crawford, and K. M. Love, "Dissolution kinetics of $CaCO_3$ in common laboratory solvents," *Journal of Sedimentary Research*, vol. 63, no. 4, pp. 641–645, 1993.

[25] R. M. Atlas, *Handbook of Media for Environmental Microbiology.* Boca Raton: Taylor & Francis, 2nd ed., 2005.

[26] K. Kimbara, T. Hashimoto, M. Fukuda, T. Koana, M. Takagi, M. Oishi, and K. Yano, "Cloning and sequencing of two tandem genes involved in degradation of 2,3-dihydroxybiphenyl to benzoic acid in the polychlorinated biphenyl-degrading soil bacterium Pseudomonas sp. strain KKS102," *J. Bacteriol.*, vol. 171, no. 5, pp. 2740–2747, 1989.

[27] M. Alkattan, E. H. Oelkers, J.-L. Dandurand, and J. Schott, "An experimental study of calcite dissolution rates at acidic conditions and 25 °C in the presence of $NaPO_3$ and $MgCl_2$," *Chemical Geology*, vol. 190, no. 1-4, pp. 291–302, 2002.

[28] A. Mucci, "Growth kinetics and composition of magnesian calcite overgrowths precipitated from seawater: Quantitative influence of orthophosphate ions," *Geochimica et Cosmochimica Acta*, vol. 50, no. 10, pp. 2255 – 2265, 1986.

[29] D. Parkhurst and C. Appelo, "User's guide to phreeqc (version 2) - a computer program for speciation, reaction-path, 1d-transport, and inverse geochemical calculations," tech. rep., US Geological Survey Water-Resources Investigation Report, 1999.

[30] B. Gao and R. S. Gupta, "Conserved indels in protein sequences that are characteristic of the phylum Actinobacteria," *Int J Syst Evol Microbiol*, vol. 55, no. 6, pp. 2401–2412, 2005.

[31] J. N. Butler, *Carbon Dioxide Equilibria and Their Applications*. Addison-Wesley, 1982.

[32] T. Perry, O. Duckworth, C. McNamara, S. Martin, and R. Mitchell, "Effects of the biologically produced polymer alginic acid on macroscopic and microscopic calcite dissolution rates," *Environmental Science and Technology*, vol. 38, pp. 3040–3046, 2004.

Chapter 4

Conclusions and Recommendations

This study establishes and refines protocols for future studies. We investigated the effects of solution composition on the extent of colonisation and growth of bacteria on Iceland Spar calcite surfaces, their metabolism and their influence on dissolution kinetics.

Results obtained in the presence and absence of phosphate and/or bacteria indicate that calcite dissolution is inhibited in the presence of bacteria and freely-available phosphate. Reduced rates of dissolution and greater degrees of surface colonisation were observed in growth media containing phosphate.

Recommendations for future studies include the use of phosphate-free media with pre-treated (adsorbed phosphate) calcite crystals over a greater number of incubation cycles. This will enable the growth of more extensive biofilm structures, akin to those observed in the presence of phosphate media. It would be interesting to develop larger batch reactors to enable increased sampling in order to monitor the dissolution kinetics. Alternatively, the use of a mixed-flow reactor in which the saturation state of the solution is fixed would be recommended, since any change in the solution composition could more readily be attributed to bacterial metabolism. Future protocols should avoid direct inoculation of reactors with weathered material but use a soil-free inoculum so as to eliminate solids that may serve as alternate surfaces for colonisation.

Appendices

Appendix A: Sample Preparation

Microbial Characterisation

PCR was introduced in 1985, as a technique that allows for the in vitro exponential amplification of genetic material This has become a basic technique that is carried out during cloning and sequencing procedures and thus was a recurring technique used in the preliminary tests conducted in this study. DNA sequencing enables the determination of the order of nucleotides on a given piece of DNA.

The limitations common to this technique include PCR bias and artefact formation. With regards to the bias, for techniques carried out in conjunction with PCR, the template to be amplified usually contains homologous genes, most commonly the 16S rRNA gene. If there is a mismatch of the primers used in amplification with the sequence of interest, or a degeneracy of the primer that prevents it from binding efficiently to the target, there will be selective amplification, equating to reduced amplification efficiency which is interpreted as a 'amplification bias. In other words, the relative abundance of homologues present in the amplified product will not be representative of the gene ratio of the template Artefacts are basically the result of single stranded DNA that has folded on itself and re-annealed.

The DNA was extracted using the PowerSoil^{TM}DNA Isolation Kit (`http://www.mobio.com/soil-dna-isolation/powersoil-dna-isolation-kit.html`) supplied by MoBio Laboratories. The concentration of the DNA was measured on a UV Ultrospec 3300 spectrophotometer . The DNA sample was amplified using PCR. The enzyme used was Taq DNA polymerase. The forward and reverse primers used were 5′ ACT CCT ACG GGA GGC AGC 3′ and 5′ GAC GGG CGG TGT GTA CAA 3′, respectively.

T-RFLP refers to Terminal Restriction Fragment Length Polymorphism and is a procedure used in profiling bacterial communities. It allows for comparative analysis of bacterial communities in a given sample. It is more of a fingerprinting technique, thus a means of determining what is present in the sample as a function of numerical dominance; fingerprinting serves to provide a global picture of the genetic structure of

the bacterial community

DNA from our field samples was extracted and purified using a commercial kit[i]. The 16S rRNAs present in the extracts are amplified using PCR (where primers specific to a desired segment of the DNA are used); the 5′ primer is labelled with a fluorescent marker. The amplicons are then cleaved using restriction enzymes. The restriction sites for each individual differ and thus the lengths of the resultant fluorescent fragments will also differ. The polymorphic fragments are then separated by electrophoresis (in this case, gel electrophoresis) and then depicted graphically in form of an electropherogram, where the generated peaks represent the abundance of a given microbial community in the sample. In essence, the lengths of the different fragments distinguish bacterial communities.

There are several limitations associated with this technique, whether as a result of human error or problems with the apparatus. Since it makes use of extraction techniques to isolate the DNA and, subsequently, PCR to amplify the DNA to a quantity sufficient for further characterisation, the limitations of both procedures affect T-RFLP. The most relevant problems are related to sizing. It is possible that digestion with restriction enzymes may not be specific enough or that incomplete digestion may occur. In addition, it is advised that all parameters be standardised so that any differences in community profiles will relate solely to the differences in phylogeny, as opposed to differences in sample preparation Artifacts, if present, may show up as false peaks on the electropherogram; note that in the T-RFLP procedure false peaks are not considered to be a problem as the DNA was digested with Mung Bean extract following PCR, so as to eliminate any artifacts that may likely have formed.

Cloning is another means of amplifying genetic material, though more time consuming and labour intensive than PCR. An added drawback of cloning coupled with sequencing is the cost of the procedure. Cloning coupled with a sequencing method, like T-RFLP, allows for microbial characterisation and, in contrast to PCR, is more a means of amplifying an already identified sequence of interest than profiling an unknown number of communities. It enables assessment of the diversity of the community in terms of the number of different species and, to a lesser extent, the relative abundance of these species. Sequencing allows a detailed identification of uncultured bacteria as well as an

[i]Mol Bio PowerSoil Kit©

estimation of their relatedness to known culturable species (*ibid*).

In this study, upon extraction and purification of DNA from the collected weathered samples, the genetic material was amplified using PCR. In accordance with a cloning kit[ii], provided vectors[iii] were spliced with the amplicons and introduced into TOP10 *E. coli* bacterial cells, which were then plated on agar with a Luria Bertani (LB) nutrient medium and allowed to proliferate. Transformed cells were selected using ampicillin resistance[iv].

[ii] Invitrogen© TOPO TA Cloning Kit©

[iii] pCR© 4-TOPO©

[iv] transformed cells will be resistant to ampicillin and will survive upon exposure

Appendix B: Additional Figures and Tables

Microbial Characteriation

Table 1: PCR Thermal Protocol

Process	**Temperature (°C)**	**Time**	**Number of Cycles**
Hot Start	94	5 min	1 ×
Pause			
Denaturation	94	1 min	30 ×
Annealing	55	30 seconds	
Elongation	72	1.5 minutes	
Extended elongation	72	8.5 minutes	1 ×
Hold	-3	hold	

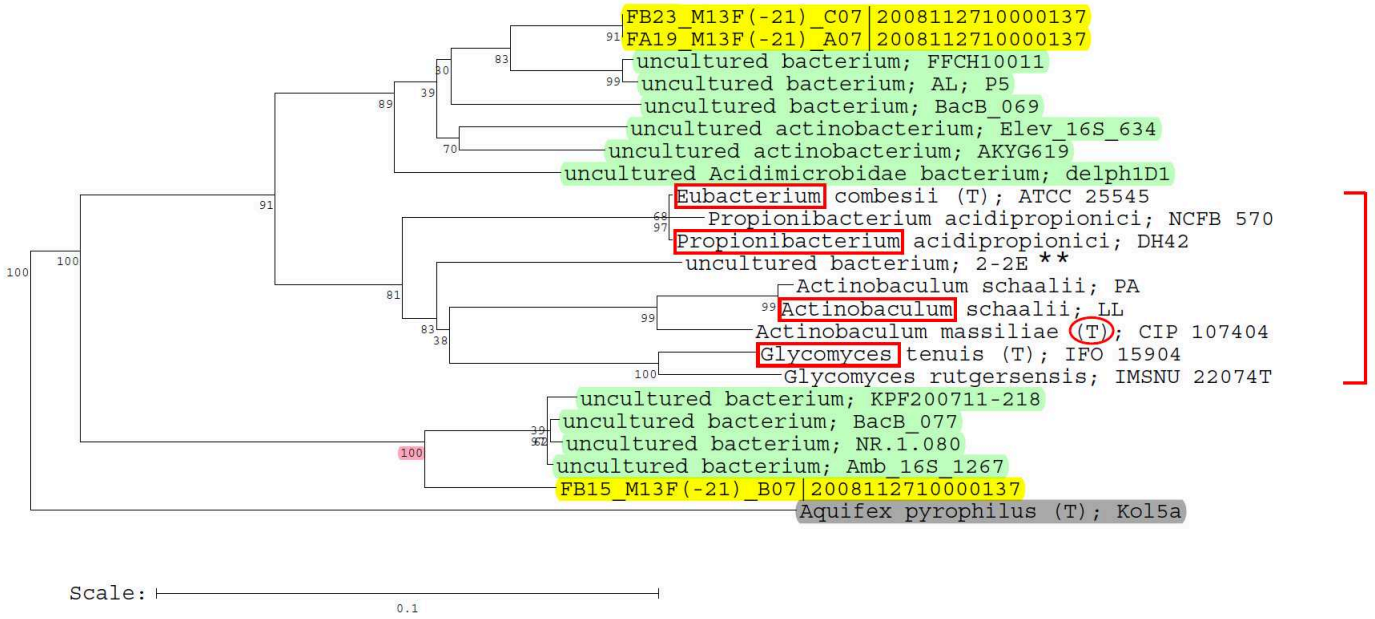

Figure 1: Phylogenetic Tree depicting cloned sequences and bacterial communities in weathered material samples.

General Characteristics of Weathered Samples and Reactor Solutions

Table 2: W-Medium recipe from Media Handbook (I = 6.6 $\times 10^{-1}$M, pH 3 $\pm$ 0.2)

Constituent	**Working Solution Mass (per L)**	**Concentration**	**Stock Solution Mass (per L)**
Sulphur	10g	0.31M	100g
KH_2PO_4	3g	0.022M	30g
$MgSO_4.7H_2O$	0.5g	2.0 $\times 10^{-3}$M	5g
$CaCl_2.2H_2O$	0.25g	1.7 $\times 10^{-3}$M	2.5g
$(NH_4)_2SO_4$	0.2g	1.5 $\times 10^{-3}$M	2
$FeSO_4.7H_2O$	10mg	3.6 $\times 10^{-5}$M	100mg

Table 3: Modified $\frac{1}{10}$ W-Medium recipe (I = 7.6 $\times 10^{-3}$M (given by PHREEQC using wateq4f.dat)) or (I = 1.4 $\times 10^{-2}$M (given by PHREEQC using llnl.dat))

Constituent	**Working Solution Mass (per L)**	**Concentration**	**Stock Solution Mass (per L)**
$NaCH_3COOH$	1g	0.012M	100g
KH_2PO_4	0.3g	0.0022M	30g
$MgSO_4.7H_2O$	0.05g	2.0 $\times 10^{-4}$M	5g
$CaCl_2.2H_2O$	0.025g	1.7 $\times 10^{-4}$M	2.5g
$(NH_4)_2SO_4$	0.02g	1.5 $\times 10^{-4}$M	2
$FeSO_4.7H_2O$	1mg (0.001g)	3.6 $\times 10^{-6}$M	100mg

Table 4: Modified $\frac{1}{10}$ W Phosphate-free Medium recipe (I = 1.1 $\times 10^{-2}$M (given by PHREEQC using wateq4f.dat)) or (I = 1.7 $\times 10^{-2}$M (given by PHREEQC using llnl.dat))

Constituent	**Working Solution Mass (per L)**	**Concentration**	**Stock Solution Mass (per L)**
$NaCH_3COOH$	1g	0.012M	100g
$MgSO_4.7H_2O$	0.05g	2.0 $\times 10^{-4}$M	5g
$CaCl_2.2H_2O$	0.025g	1.7 $\times 10^{-4}$M	2.5g
$(NH_4)_2SO_4$	0.02g	1.5 $\times 10^{-4}$M	2
$FeSO_4.7H_2O$	1mg (0.001g)	3.6 $\times 10^{-6}$M	100mg

A

X-Ray Fluorescence Major Element Analytical Package

Mucci/Sulu-Gambari

Sample	SiO2	TiO2	Al2O3	Fe2O3	MnO	MgO	CaO	Na2O	K2O	P2O5	BaO	Ce	Co	Cr2O3	Cu	Ni	Sc	V	Zn	LOI	Total	Lab No.
FA - 5He 1	50,72	0,2884	10,13	2,4025	0,0555	1,31	16,22	2,1253	1,88	0,156	634,5	33	<d/l	90,0	24	16	13	47,2	8	14,64	100,02	10-001
FB - 5He 3	53,76	0,6174	13,17	4,8954	0,1299	4,73	11,89	2,8522	4,71	1,039	1936,7	80	12	126,9	37	26	21	104,3	45	2,32	100,36	10-002
Detection Limits (ppm):	60	25	120	25	25	95	15	35	25	35	12	15	10	10	2	3	10	7	2	100		

Note: The results are expressed as weight percent, the trace elements (BaO to Zn) as ppm (ug/g).

Total iron present has been recalculated as Fe2O3. In cases where most of the iron was originally in the ferrous state (usually the case with unaltered rocks) a higher total is the result.

Analyses done on fused beads prepared from ignited samples.

Detection limits are based on three times the background sigma values.

"int" indicates that there is interference from unusually high quantities of other trace elements.

B

CO2 analysis

Mucci/Sulu-Gambari

Sample	CO2 (%)	Lab No.
FA - 5He 1	11,83	10-001
FB - 5He 3	1,72	10-002
Detection Limits(%):	0,01	

Note: The samples were analyzed using an ELTRA CS-800 automated analyzer.

CO2 results reported on dry weight samples.

Detection limits are based on three times the background sigma values.

Figure 2: Results of (A) XRF and (B) total carbon analyses of weathered material samples from sites 1 (FA) and 2 (FB).

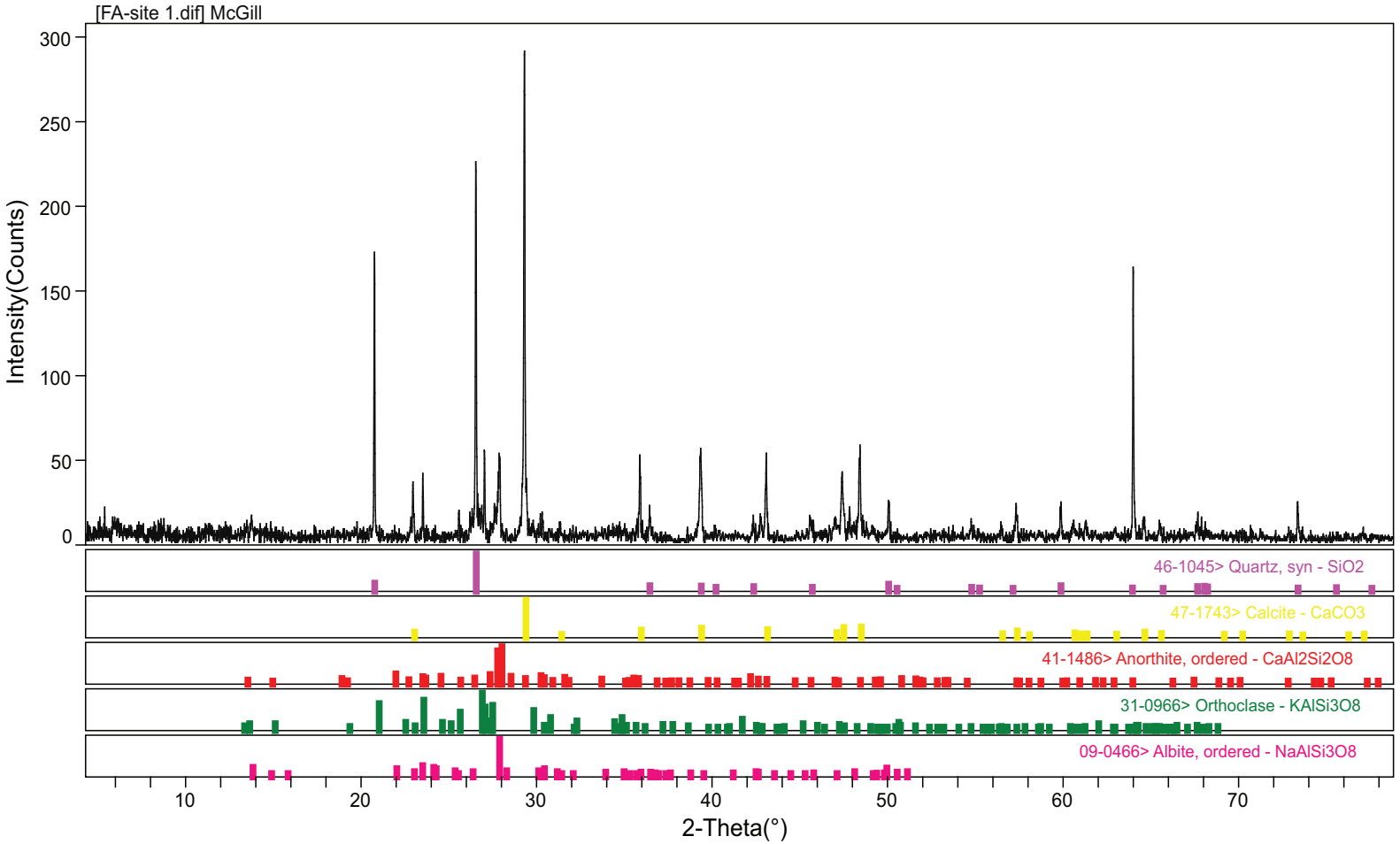

Figure 3: X-ray diffractogram of weathered material samples from first site with calcite peak at $29\,^{\circ}2 - theta$

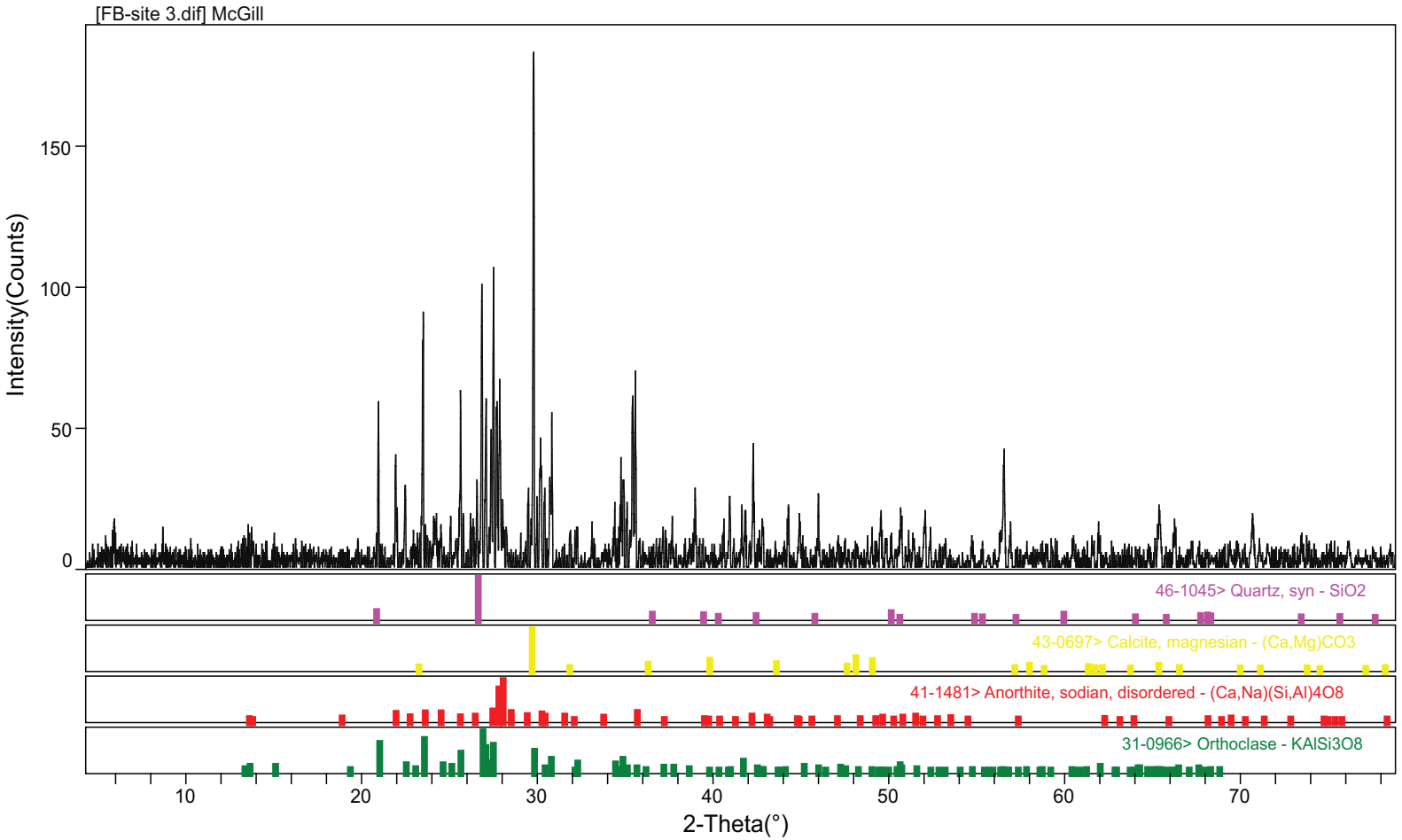

Figure 4: X-ray diffractogram of weathered material samples from first site with calcite peak at $29\,^{\circ}2 - theta$

Table 5: Carbonate-free Trace Metal Solution Recipe (I = 1.7 $\times 10^{-5}$M)

Constituent	**Working Solution Mass/Volume (per L)**	**Concentration**	**Stock Solution Mass (per L)**
$MgSO_4.7H_2O$	0.01g	4 $\times 10^{-5}$M	0.01g
$FeSO_4.7H_2O$	0.095mg (0.000095g)	3.4 $\times 10^{-7}$M	0.95mg
$ZnSO_4.7H_2O$	0.144mg (0.000144g)	5.01 $\times 10^{-7}$M	1.44mg
$CuSO_4.5H_2O$	0.025mg (0.000025g)	1.0 $\times 10^{-7}$M	0.25mg
$CoSO_4.7H_2O$	0.028mg (0.000025g)	10 $\times 10^{-8}$M	0.28mg
H_3BO_3	0.006mg (0.000006g)	10 $\times 10^{-8}$M	0.06mg
Conc acid (H_2SO_4)	51.3μL		